

The fundamental localization phases in quasiperiodic systems: A unified framework and exact results

Xin-Chi Zhou,^{1,2} Bing-Chen Yao,¹ Yongjian Wang,³
Yucheng Wang,^{4,5,6} Yudong Wei,^{1,2} Qi Zhou,⁷ and Xiong-Jun Liu^{1,2,5,*}

¹*International Center for Quantum Materials and School of Physics, Peking University, Beijing 100871, China*

²*Hefei National Laboratory, Hefei 230088, China*

³*School of Mathematics and Statistics, Nanjing University of Science and Technology, Nanjing 210094, China*

⁴*Shenzhen Institute for Quantum Science and Engineering, Southern
University of Science and Technology, Shenzhen 518055, China*

⁵*International Quantum Academy, Shenzhen 518048, China*

⁶*Guangdong Provincial Key Laboratory of Quantum Science and Engineering,
Southern University of Science and Technology, Shenzhen 518055, China*

⁷*Chern Institute of Mathematics and LPMC, Nankai University, Tianjin 300071, China*

The disordered quantum systems host three types of quantum states, the extended, localized, and critical, which bring up various distinct fundamental phases, including the pure phases and coexisting ones with mobility edges. The quantum phases involving critical states are of particular importance, but are less understood compared with the other ones, and the different phases have been separately studied in different quasiperiodic models. Here we propose a unified framework based on a spinful quasiperiodic system which unifies the realizations of all the fundamental Anderson phases, with the exact and universal results being obtained for these distinct phases. Through the duality transformation and renormalization group method, we show that the pure phases are obtained when the chiral symmetry preserves in the proposed spin-1/2 quasiperiodic model, which provides a criterion for the emergence of the pure phases or the coexisting ones with mobility edges. Further, we uncover a new universal mechanism for the critical states that the emergence of such states is protected by the generalized incommensurate matrix element zeros in the spinful quasiperiodic model, as a nontrivial generalization of the mechanism in the spinless systems. We also show with the Avila's global theory the criteria of exact solvability for the present unified quasiperiodic system, with which we identify several new quasiperiodic models hosting exactly solvable Anderson phases. We particularly reach two novel models, with one hosting all basic types of mobility edges and the other hosting all the seven fundamental phases of Anderson localization. Finally, an experimental scheme is proposed to realize these models using quasiperiodic optical Raman lattices. This study establishes a profound theoretical framework which enables an in-depth exploration of the broad classes of all fundamental localization phases in quasiperiodic systems, and offers key insights for constructing their exactly solvable models with experimental feasibility.

I. INTRODUCTION

Anderson localization, wherein quantum states localize exponentially in real space due to disorder-induced scattering, is a fundamental and universal phenomenon in disordered systems [1–4]. It manifests distinctly across two categories of aperiodic systems: disordered systems and quasiperiodic lattices. In disordered systems, scaling theory predicts that noninteracting states are localized in one and two dimensions even under weak disorder, whereas in three dimensions, an Anderson transition from extended to localized states occurs only with sufficiently strong disorder [5]. In contrast, quasiperiodic (QP) lattices exhibit richer physics including Anderson transitions in all spatial dimensions, governed by quasiperiodic parameters [6, 7]. Importantly, both extended and localized states can coexist within a single quantum phase, separated by characteristic energies known as mobility edges (MEs) [8–36]. The ability to derive exact analytical expressions for characteristic length

scales and MEs in various QP models [19, 25, 37–39] plays a crucial role in advancing the fundamental understanding of localization transitions, providing theoretical insights that extend beyond numerical simulation.

Between the extended and localized states lie the critical states, which are delocalized in both position and momentum spaces. Critical states have recently attracted extensive research interests [37–65] due to their unique properties, such as local scale invariance, multifractality, and critical quantum dynamics. Recent advances, particularly through Avila's global theory [37, 66], refine a rigorous characterization [67, 68] of the critical states, showing that critical states generally arise when the hopping couplings in a QP system are non-uniform and possess incommensurately distributed zeros (IDZs) in the thermodynamic limit [69]. The exact theory enables unambiguous determination of critical phases and the new MEs between critical and other states [37]. Furthermore, this rigorous characterization of critical states provides a well-defined foundation for incorporating many-body interactions, thereby extending the paradigm of criticality beyond the single-particle picture. Inclusion of interactions further enriches the physics of the critical

* xiongjunliu@pku.edu.cn

phase, with multifractality of the wave function influencing both ground state properties associated with symmetry breaking [69–74] and the emergence of many-body critical (MBC) phases [47, 75] at infinite temperature. The MBC phase, interpolating the thermal phase and many-body localization (MBL) [76–82], signifies a non-ergodic but delocalized regime that violates the eigenstate thermalization hypothesis (ETH) [83–86].

The recently developed quasiperiodic mosaic lattice models [19, 33, 37, 58] and their generalizations [27, 30, 32, 54, 60, 87] advance the rigorous characterization of all eigenstates in the spectra through the analytical study of their localization properties (Lyapunov exponent or LE) using Avila’s global theory [66]. With the mosaic models, the MEs can also be analytically obtained. On the other hand, while the various exactly solvable models are proposed, these different models are treated on a case-by-case basis. There is no unified theory showing that under what conditions a generic exactly solvable model undergoes phase transitions between the pure localized, extended, and critical phases without MEs, and otherwise it possesses MEs that separate these states, i.e., the transitions are energy-dependent. Besides, Avila’s global theory enables an analytic study of the spinless models with nearest-neighbor hopping, while the exact results for more complicated systems are scarce, hindering the in-depth understanding of the localization physics in more generic systems. For instance, the universal mechanism for critical states in the complex systems with internal degrees of freedom, such as spins, remains unknown. Addressing these issues is not only important in fundamental theory, but also of high significance in experiment, as the remarkable experimental progresses in engineering the spin and orbital degrees of freedom [88–96] have enabled the realization of complex QP systems beyond toy models. These crucial fundamental issues motivate us to establish a universal theory that can generically characterize spinful QP lattice systems without relying on specific microscopic details.

A. Summary of results

In this work, we propose to investigate the generic spin-1/2 quasiperiodic (QP) system, with which we establish a unified theoretical framework for all fundamental localization phases based on the exact and universal results uncovered in this system. The proposed generic QP framework not only unifies existing 1D spinful QP models with exact analytical solutions, but also encompasses spinless QP models through an additional Majorana representation. More importantly, this system establishes a versatile platform for constructing new exactly solvable QP models exhibiting rich phase structures, including pure phases and coexisting phases with MEs.

The universal results are obtained in this unified framework and can be summarized as follows. First, we show with duality transformation and renormalization group

method that the pure extended, localized, or critical phases are obtained when the system preserves a chiral symmetry. Accordingly, the emergence of coexisting phases with MEs necessitates to break the chiral symmetry. Second, we unveil a new universal mechanism for critical states in the spinful quasiperiodic system, which arise from generalized incommensurate zeros (GIZs) in matrix elements. This mechanism is a nontrivial generalization of the incommensurate hopping zeros in the spinless QP models, enabling a much broader pathway of realizing and characterizing the critical states. Third, we establish the exactly solvable condition, under which the 1D spinful QP system can be transformed into effectively spinless QP models of dressed particles, and then can be exactly solved. This result provides a powerful guiding principle to construct exactly solvable models that host a variety of novel localization physics, particularly the models encompassing all basic types of MEs and all seven fundamental phases in localization physics.

B. Organization of the work

The remainder of the paper is organized as follows. In Sec. II, we introduce the generic framework for 1D spinful QP chains, including the basic Hamiltonian and the analytical approaches employed in this study, such as dual transformations, renormalization group methods, and Avila’s global theory. In Sec. III, we present the universal results for the spinful QP chains, as organized into three theorems shown here. These universal results serve as guiding principles for constructing multiple exactly solvable models hosting distinct classes of localization physics and anomalous MEs, including a novel model that realizes the seven fundamental phases of Anderson localization in Sec. IV. In Sec. V, we propose an experimental scheme for the realization of these new models using a generic quasiperiodic optical Raman lattice. Finally, we conclude in Sec. VI, with additional details and proofs provided in Appendix.

II. GENERIC FRAMEWORK

A. The spinful quasiperiodic model

We begin with the generic one-dimensional (1D) spin-1/2 quasiperiodic system, whose Hamiltonian is given by

$$H = \sum_{j,s,s'} (c_{j+1,s}^\dagger \Pi_j^{s,s'} c_{j,s'} + \text{h.c.}) + \sum_{j,s,s'} c_{j,s}^\dagger M_j^{s,s'} c_{j,s'}, \quad (1)$$

where $c_{j,s}^\dagger (c_{j,s})$ creates (annihilates) a particle on site j with (pseudo)spin $s = \uparrow, \downarrow$ that can denote real spin, sublattices or particle-hole. This model includes two key ingredients, as illustrated in Fig. 1(a). First, the hopping coupling matrix $\Pi_j = \sum_l p_j^l \sigma_l$, as written in terms of Pauli matrices σ_l with $l = \{0, x, y, z\}$, represents the

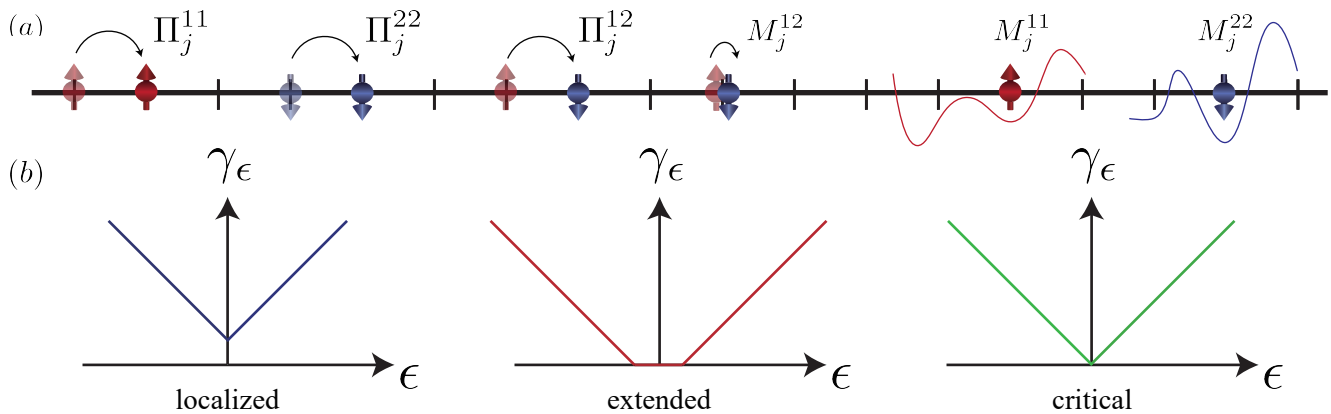


Figure 1. Illustration of generic framework. (a) The different processes of the spinful quasiperiodic systems. The hopping coupling matrix $\Pi_j^{s,s'}$ denote the momentum transfer coupling with the diagonal (off-diagonal) terms for the same (different) internal degrees of freedom. The on-site matrix $M_j^{s,s'}$ represents the on-site spin flipped and on-site modulation of the system. (b) The conditions when the Avila's global theory can give rise to the analytical characterization of the (reduced) 1D quasiperiodic chain. The nonzero acceleration of the complexified Lyapunov exponent γ_ϵ is quantized to the unique integer: $d\gamma_\epsilon/d\epsilon = 2\pi\mathbb{Z}$. Then the original Lyapunov exponent can be obtained by the expression obtained from the $\epsilon \rightarrow \infty$.

spin-independent (for $l = 0$) and the spin-dependent (for $l = x, y, z$) hopping coupling terms. The latter includes both the spin-conserved ($l = z$) and spin-flip ($l = x, y$) hopping terms, corresponding to the spin-orbit coupling in the periodic systems. Second, the onsite matrix $M_j = \sum_l m_j^l \sigma_l$ also involves the spin-independent chemical potential and the Zeeman coupling terms. The coefficients $p_j^l = t^l + \mu^l V_j^{\text{od}}$ and $m_j^l = \lambda^l + V^l V_j^{\text{d}}$, where $(t^l, \lambda^l, \mu^l, V^l)$ are constants, the off-diagonal quasiperiodic modulation $V_j^{\text{od}} = \cos[2\pi\alpha(j + 1/2) + k_y]$ and the diagonal quasiperiodic modulation $V_j^{\text{d}} = \cos(2\pi\alpha j + k_y)$. Here $\alpha = \lim_{n \rightarrow \infty} (F_{n-1}/F_n) = (\sqrt{5} - 1)/2$ is an irrational number approached by the Fibonacci sequence F_n , and k_y is a constant phase factor. In this work, we take that the quasiperiodic term has a single frequency. To facilitate our discussions, we define the combinations of the Pauli matrices σ_l as $\sigma_\pm = (\sigma_x \pm i\sigma_y)/2$ and $\Lambda_\pm = (\sigma_z \pm \sigma_0)/2$.

This spinful QP system unifies various QP models, including the existing 1D spinful models with analytical solutions, and spinless models by taking the Majorana representation (see the details in Appendix A and Appendix E). More importantly, with this unified framework we shall develop a series of new and exactly solvable models which host various novel quantum phases with or without mobility edges. Below, we outline the three main theoretical approaches employed in this study.

B. Dual transformation

The dual transformation is a non-local operation similar to the Fourier transformation, and maps the system between real space and dual momentum space. It is defined as $c_{j,s} = (1/\sqrt{L}) \sum_n e^{-i2\pi n\alpha j} c_{n,s}$. The extended,

localized, and critical states behave differently under this transformation. For an extended state, the wave function is delocalized in real space, but localized in dual momentum space, whereas the localized state is delocalized in dual momentum space but localized in real space. These opposing features are exchanged under the dual transformation. In contrast, critical states exhibit behavior distinct from the other two; they remain delocalized in both real and dual spaces, and are invariant under the transformation. For example, when the system has a QP hopping term ($V_j^{\text{od}} a_j^\dagger a_{j+1} + \text{h.c.}$), which dominates over other hopping couplings and is invariant under the dual transformation due to the presence of incommensurately distributed zeros (IDZs) in the QP hopping modulation V_j^{od} , the critical states may emerge and exhibit self-dual for having incommensurate nodes corresponding to the IDZs [37, 69]. These incommensurate nodes in the delocalized wave functions remain unchanged under the dual transformation, driving the delocalized states into critical states. An intuitive picture suggests that IDZs partition the 1D system into multiple segments, where the wave function reorganizes, exhibiting a self-similar pattern characteristic of the critical states.

The distinct behaviors of the three types of states can be mapped onto a 2D system to get an intuitive physical interpretation, where x - and y -axes correspond to the real and dual spaces, and the dual transformation exchanges the two axes. In this mapping, the extended state is delocalized along x -direction and localized along y -direction, and the opposite is true for localized states. The critical state is delocalized in both directions. Thus, the swapping of the two axes transforms the localized and extended states, while leaving the critical states unchanged. We use 1D spinless 1D extended Aubry-André (EAA) model [40, 41, 44] as an example,

which is characterized by the nearest-neighbor hopping $t_j = t + \mu V_j^{\text{od}}$ and on-site potential $V_j = V_0 V_j^{\text{d}}$ (see details in Appendix A). By interpreting the phase shift k_y as the quasi-momentum in the y -direction and performing a Fourier transformation, the 1D spinless EAA model maps to a 2D Hofstadter model that describes a particle moving in a magnetic field [97, 98]. In this mapping, the uniform hopping terms correspond to hopping in the x -direction, while the on-site potential $V_j^{\text{d}} a_j^\dagger a_j$ corresponds to the hopping in the y -direction with a magnetic flux $\exp(i2\pi\alpha x) a_{x,y}^\dagger a_{x,y+1} + \text{h.c.}$. Similarly, the QP hopping term ($V_j^{\text{od}} a_j^\dagger a_{j+1} + \text{h.c.}$) represents diagonal hopping in the 2D plane under the magnetic flux. The relative hopping amplitude shapes the cyclotron orbits while maintaining the flux within each orbit. When the hopping in the x - or y -direction dominates, the extended or localized states emerge. In contrast, when the hopping in diagonal direction dominates, hence having equal weight in both directions, the critical states are resulted and exhibit delocalized feature in both axes.

C. Renormalization group

The renormalization group (RG) approach [99–107] investigates the relevance of renormalized coefficients by iterating the rational approximations of the QP parameter. Specifically, one takes a rational sequence $\alpha^{(n)} = p_n/q_n$ to define a sequence of periodic Hamiltonians $H^{(n)}$, which approach the quasiperiodic regime only at the irrational limit $\alpha = \alpha^{(\infty)}$. The RG flow to $n \rightarrow \infty$ determines the properties of the states at quasiperiodic regime. With the rational sequence, the energy dispersion of $H^{(n)}$ is a periodic function of quasi-momenta κ_x and κ_y . To systematically investigate how the relevant coefficients flow as the system size increases, we compute the characteristic determinant $P^{(n)} = |\mathcal{H}^{(n)} - E|$ at a target energy E for a given size $L = F_n$, which is given by

$$\begin{aligned} P^{(n)}(E; \kappa_x, \kappa_y) &= t_R^{(n)} \cos(\kappa_x + \kappa_x^0) + V_R^{(n)} \cos(\kappa_y + \kappa_y^0) \\ &+ \mu_R^{(n)} \cos(\kappa_x + \tilde{\kappa}_x^0) \cos(\kappa_y + \tilde{\kappa}_y^0) \\ &+ \epsilon_R^{(n)}(E, \varphi, \kappa) + T_R^{(n)}(E), \end{aligned} \quad (2)$$

where $\epsilon_R^{(n)}$ represents irrelevant higher harmonic terms. The asymptotic nature of eigenstates at $n \rightarrow \infty$ is determined by comparing the relative magnitudes of renormalized hopping coefficients. For extended states, the dominant hopping is along x direction, yielding $|\mu_R^{(n)}/t_R^{(n)}|, |V_R^{(n)}/t_R^{(n)}| \rightarrow 0$. For localized states, the dominant hopping is along y direction, leading to $|t_R^{(n)}/V_R^{(n)}|, |\mu_R^{(n)}/V_R^{(n)}| \rightarrow 0$. For critical states, all three hopping coefficients are equally relevant, such that $|\mu_R^{(n)}/V_R^{(n)}|, |\mu_R^{(n)}/t_R^{(n)}| \geq 1$. With the RG flow we can determine the transitions between extend, localized and critical phases, and the mobility edges as the energy dependent transition points.

D. Avila's global theory

When the Hamiltonian in Eq. (1) can be reduced to an effectively spinless quasiperiodic (QP) chain of dressed particles, the system can be analytically characterized using Avila's global theory [66]. This theory enables the analytical calculation of the Lyapunov exponent (LE), which is the inverse of the localization length. The method provides a rigorous characterization of extended, localized, and critical states. Specifically, the non-negative LE $\gamma(E)$, quantifies the localization properties of eigenstates with energy E . If $\gamma(E) > 0$, the state has a finite localization length $\xi(E) = \gamma^{-1}(E)$. If $\gamma(E) = 0$, the state is delocalized, with a divergent localization length, corresponding to either an extended or a critical state. Critical states arise when the transfer matrix T_j of the delocalized states becomes singular [67, 68]. This singularity can emerge from a universal physical mechanism that the hopping couplings have IDZs [37], or the QP potential has incommensurately distributed divergence points, which effectively divides the system into infinite segments, acting as IDZs.

Furthermore, Avila's global theory can also be employed to derive the analytical expression for the correlation length of extended states. This is achieved by performing the transformation of the system into dual space. Then one can calculate the localization length of localized states in the dual space, which is equivalent to the correlation length of the corresponding extended states in the real space.

Now we outline the procedure for obtaining the LE using Avila's global theory. For the generic 1D spinful QP Hamiltonian in Eq. (1), we consider the 4-by-4 transfer matrix T_j given by $(u_{j+1\uparrow}, u_{j+1\downarrow}, u_{j\uparrow}, u_{j\downarrow})^\top = T_j(u_{j\uparrow}, u_{j\downarrow}, u_{j-1\uparrow}, u_{j-1\downarrow})^\top$, where $u_{j\sigma}$ is the wave function of eigenstate at site j with spin σ . In general, the 4-by-4 transfer matrix does not guarantee exact solvability. Exact solvability arises when the transfer matrix is reduced to a block-diagonal 2-by-2 form. As we shall show in Sec. III C, the present spinful system can be reduced to effective spinless QP model of dressed particles when certain local constraint is introduced. Consequently, the effective transfer matrix becomes a 2-by-2 matrix. In this regime, the LE $\gamma_\epsilon(E)$ is computed as

$$\gamma_\epsilon(E) = \lim_{n \rightarrow \infty} \frac{1}{2\pi n} \int \ln \|\mathcal{T}_{n,1}(\theta + i\epsilon)\| d\theta. \quad (3)$$

Here, E is the energy of the corresponding eigenstate, $\|A\|$ is the norm of the matrix A , i.e. the square root of the largest eigenvalue of $A^\dagger A$, $\mathcal{T}_{n,1} = \prod_{j=1}^n T_j$. The ϵ is the imaginary part of complexified quasiperiodic phase shift $\theta + i\epsilon$. The LE is generally challenging to compute analytically, even for the simple 2-by-2 transfer matrix T_j . Nevertheless, a key result from Avila's global theory is that with the complexification one can analytically compute the LE for all eigenstates, as long as the LE $\gamma_\epsilon(E)$ is convex, continuous and piecewise linear with

quantized right-derivative, given by

$$\lim_{\epsilon \rightarrow 0^+} \frac{1}{2\pi\epsilon} [\gamma_\epsilon(E) - \gamma_0(E)] = \mathbb{Z}. \quad (4)$$

In this case, the nonzero part of derivative of LE is quantized to an integer for all range of ϵ : $d\gamma_\epsilon/d\epsilon = 2\pi\mathbb{Z}$. This condition also implies that there is no turning point before γ_ϵ intersects the x - or y -axis, as illustrated in Fig. 1(b). This has an important consequence that the analytic expression for the LE can be determined in the following way: one first computes the complexified LE γ_ϵ at the limit $\epsilon \rightarrow \infty$, which can be obtained straightforward. Then, using the properties that $\gamma_\epsilon(E)$ is convex, continuous, and piecewise linear with a quantized right-derivative, the analytic expression of the LE determined at $\epsilon \rightarrow \infty$ can be extended to all values of ϵ . Finally, the exact LE is obtained by taking back $\gamma_{\epsilon=0}$, which represents the original physical Lyapunov exponent that characterizes the properties of all eigenstates.

III. UNIVERSAL RESULTS FOR THE QUASIPERIODIC SPINFUL CHAINS

In this section, with the theoretical approaches introduced above, we show three universal results for the spinful quasiperiodic systems, which facilitates to establish a unified framework of all the fundamental localization phases, as summarized in Fig. 2. First, we prove a generic condition under which mobility edges (MEs) disappear in the system, namely, the pure phases are obtained under this condition. Second, we uncover a new universal mechanism that critical states are protected by the generalized incommensurate zeros in matrix elements. Third, we outline the conditions, under which the Avila's global theory can be applied to obtain analytic solutions to the localization properties, correlation length, the associated phase transition points, and mobility edges.

A. Criteria for pure phases without MEs

We firsts show that the system hosts only pure phases without MEs under the following conditions: *The on-site matrix M_j are purely quasiperiodic, and the hopping coupling matrix Π_j are either uniform or purely quasiperiodic, with the system satisfying the chiral symmetry*

$$\sigma_y \Pi'_j \sigma_y^\dagger = -\Pi'_j, \quad \sigma_y M'_j \sigma_y^\dagger = -M'_j. \quad (5)$$

We show this criterion by proving that all leading coefficients in Eq.(2) are energy-independent, ensuring that the transitions between different types of states are energy independent, and consequently, the system exhibits pure phases without MEs [Fig.2(a)]. For convenience. we transform Π'_j and M'_j into the local bases such that the on-site coupling matrix is diagonal, given explicitly as

$$\Pi'_j = p_j^\perp \sigma_x + p_j^z \sigma_z, \quad M'_j = m_j^z \sigma_z, \quad (6)$$

The proof follows from a careful power counting analysis of the energy dependence in characteristic polynomial $P(E; \kappa_x, \kappa_y)$ in Eq. (2). We consider an odd system size L without loss of generality. Due to chiral symmetry, eigenenergies appear in pairs $(-E, E)$, and therefore $P(E)$ is an even function of energy E . In the power counting analysis, the energy E explicitly contributes a power of E , while p_j^\perp and p_j^z contribute dispersions of e^{ik_x} , and m_j contributes dispersions of e^{ik_y} (with the mapping to 2D system). Here $\kappa_x = Lk_x$ and $\kappa_y = Lk_y$. We utilize the periodic structure to simplify the power counting. Thus, the characteristic polynomial can be expressed as the determinant of a $2L \times 2L$ matrix $|A(E)|$ (details in Appendix B), with elements

$$A_{mj} = e^{i2\pi\alpha jm} \left[m_j \sigma_0 + a_{k_x, k_y}^{11} \Lambda_+ + a_{k_x, k_y}^{22} \Lambda_- - E \sigma_x \right], \quad (7)$$

where

$$a_{k_x, k_y}^{11(22)} = t_{j-1}^{+(-)} e^{-i(2\pi\alpha m + k_x)} + c.c., \quad (8)$$

and $t_j^\pm = p_j^z \pm ip_j^\perp$. This structure ensures the energy terms and momentum dispersions decouple naturally, eliminating cross terms such as Ee^{ik_x} . Below, we analyze separately the dominant dispersions for extended, localized, and critical states.

For the extended and localized states, characterized by dispersions of the form $\cos n_x Lk_x$ and $\cos n_y Lk_y$, respectively, where $n_x, n_y \geq 1 \in \mathbb{Z}$, we show that the dominating coefficients are energy-independent. Specifically, the leading dispersion $\cos Lk_x$ and $\cos Lk_y$ vanish due to chiral symmetry, as these terms arise from the product of L factors of e^{ik_x} and L factors of energy E , yielding an odd power of energy $E^L \cos Lk_x(k_y)$, which is forbidden. Thus, the dominant terms become $\cos 2Lk_x$ and $\cos 2Lk_y$, whose coefficients are energy-independent, solely given by diagonal elements of the determinant, leaving no opportunity to involve E -dependent terms. Therefore, transitions for extended and localized states do not depend on energy, implying the absence of MEs.

For the critical states, characterized by dispersions of the form $\cos n_x Lk_x \cos n_y Lk_y$ with $n_x, n_y \geq 1 \in \mathbb{Z}$, we show below that they are energy independent. We consider two distinct scenarios for the chiral symmetry: uniform and purely quasiperiodic hopping matrices Π_j , with M_j always purely quasiperiodic (details in Appendix B).

In the first scenario, for the uniform Π_j , the leading dispersion $\cos Lk_x \cos Lk_y$ emerges from products of exactly L factors of p_j (each contributing e^{ik_x}) and L factors of m_j (each contributing e^{ik_y}). Thus the momentum terms are exhausted, leaving no momentum dependence of the coefficients, namely, being energy-independent.

In the second scenario, where both Π_j and M_j are purely quasiperiodic, the leading dispersions include terms such as $\cos 2Lk_x \cos Lk_y$, $\cos Lk_x \cos 2Lk_y$, and $\cos 2Lk_x \cos 2Lk_y$ [108], all of which are energy-independent. The dispersion $\cos Lk_x \cos 2Lk_y$ arises from product of L factors of p_j (each contributing $e^{ik_x} e^{ik_y}$)

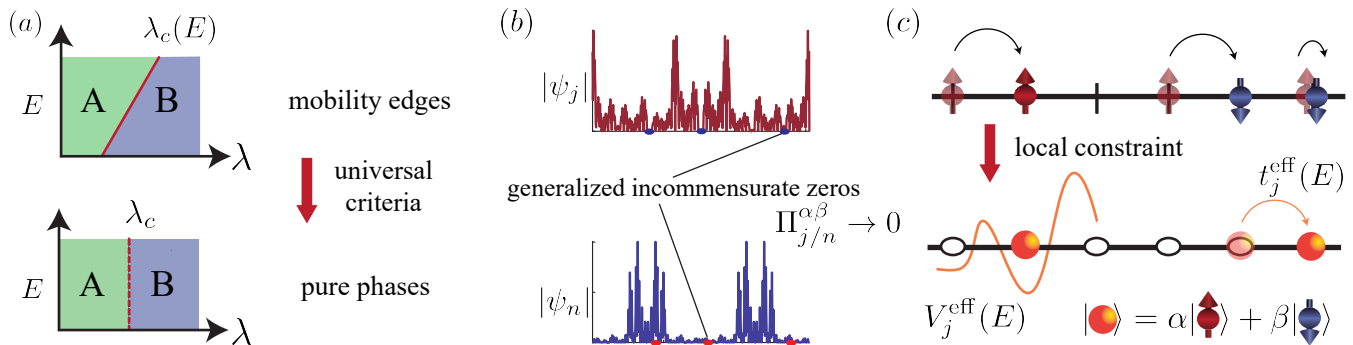


Figure 2. Three universal results for the spinful quasiperiodic chains. (a) Criteria for the system to exhibit pure phases without mobility edges. Here, λ is the tuning parameter and E is the energy. States A and B refer extended, localized, or critical states. The energy-dependent transition points $\lambda_c(E)$ become energy-independent, denoted as λ_c , indicates transitions from a regime mobility edges (MEs) to a pure phase without MEs. (b) Mechanism for the emergence of critical states in the 1D spinful quasiperiodic (QP) system, generated by dual-invariant generalized incommensurate zeros (GIZs) in matrix elements, marked as the blue and red circles in real and dual spaces. (c) Exact solvability of QP systems from local constraint. The local constraint that reduces the generic 1D spinful QP chain into a 1D spinless QP chain of dressed particles (represented by orange spheres), with energy-dependent or independent nearest-neighbor hopping coefficients $t_j^{\text{eff}}(E)$ and on-site potentials $V_j^{\text{eff}}(E)$, rendering the system can be exactly solved through Avila's global theory.

and L factors of m_j (each contributing e^{ik_y}), containing exactly $2L$ factors, and thus remains free of energy-dependent contributions. Similarly, the other two dispersions originate from product of $2L$ factors of p_j (each contributing $e^{ik_x} e^{ik_y}$), which generically lead to both $\cos 2Lk_x \cos Lk_y$ and $\cos 2Lk_x \cos 2Lk_y$ [109], whose coefficients are both energy-independent. Consequently, critical states also exhibit energy-independent transitions, eliminating the presence of MEs.

The proof of the criterion highlights the crucial role of chiral symmetry in excluding MEs for the present spinful quasiperiodic systems. It therefore provides general guidelines for realizing pure phases without MEs, as well as coexisting phases with MEs. For coexisting phases, one way to realize is to directly break the condition by adding higher QP frequencies to the system. Alternatively, one may break the chiral symmetry of the system by introducing spin-conserved hopping terms or QP chemical potential into the Hamiltonian [110].

B. Universal mechanism for the emergence of critical states

We further show a new universal mechanism for the critical states in spinful QP chains: *Spinful quasiperiodic systems can host critical states if the system possesses generalized incommensurate matrix element zeros \mathcal{G}_{Π}* , which are defined by

$$\mathcal{G}_{\Pi} = \left\{ j_k \left| \lim_{L \rightarrow \infty} \Pi_{j_k}^{\alpha\beta} = 0 \right. \right\}, \quad (9)$$

where $\alpha, \beta \in \{1, 2\}$ label the matrix element indices. The generalized incommensurate zeros (GIZs) in the above equation refer to the IDZs for any component of the hopping coupling matrix Π_j in the thermodynamic limit.

This is a nontrivial generalization of the mechanism for critical states in spinless QP chains [37] to the present spinful systems. In spinless systems, the IDZs partition the system into multiple segments, driving the delocalized wave function to reorganize and develop the characteristic self-similar structure of critical states [37, 69]. In the current spinful systems, the dual-invariant GIZs will similarly partition system into incommensurately distributed segments in the internal degree of freedom (spin) and the real space, leading to critical states with multifractal features [Fig. 2(b)]. When the QP hopping matrix Π_j with GIZs dominates over the on-site QP couplings M_j , the critical states emerge.

We can also show this result by mapping the spinful QP model to a generalized 2D bilayer square lattice system, in the presence of an external magnetic field with an irrational flux threading each unit cell. The QP hopping term $V_j^{\text{od},ss'} c_{j+1s}^{\dagger} c_{js'} + \text{h.c.}$ with GIZs in the Hamiltonian characterizes the intra-layer (for $s = s'$) or inter-layer (for $s \neq s'$) hopping coupling in the diagonal direction. In contrast, the uniform hopping matrix elements and the onsite terms are mapped to the corresponding couplings along x and y directions, respectively (See Appendix C for details). When the QP hopping dominates over other terms, the cyclotron motion is extended in the diagonal direction, leading to delocalization in both directions (the real space and dual space). The resulted states then exhibit self-duality, the key feature of critical states.

In addition to the GIZs, we present a secondary guiding principle to realize critical states in spinful QP chains by connecting the spinful system to the spinless QP models. In particular, when the on-site matrix M_j has IDZs in the matrix component which is shared by the hopping term Π_j , one can reduce the spinful QP chain to an effective 1D spinless model, with the IDZs in M_j being

transferred into either IDZs in the hopping coefficients or into incommensurately distributed divergence points in the on-site potentials. We therefore reduce to the universal mechanism in the spinless system for generating the critical states. For instance, when $\Pi_j \sim t\sigma_+$ is uniform, critical states emerge if M_j host IDZs in its σ_x or σ_y coefficients. We shall show this principle through the quasiperiodic mosaic models and the new exactly solvable models proposed in the next subsection.

The GIZs \mathcal{G}_Π and the IDZs in the matrix component of M_j shared in Π_j serve as two guiding principles for introducing critical orbitals into the spectrum. These principles, together with the criteria for pure phases, provide powerful insights for constructing spinful QP models that host all the fundamental localization phases.

C. Exact solvability of QP systems from local constraint

We now present the third universal result regarding exact solvability of the spinful QP system: *A spinful quasiperiodic system can have exactly solvable points if the hopping coupling matrix Π_j or its dual counterpart $\tilde{\Pi}_n$ are degenerate, which corresponds to*

$$\det |\Pi_j| = 0 \quad \text{or} \quad \det |\Pi_n| = 0, \quad (10)$$

together with p_j^s and off-diagonal terms of M_j being either constant or purely quasiperiodic. This condition represents a local constraint, where the spinful QP systems can be reduced to an effectively 1D spinless QP chain for the *dressed particle* with only nearest-neighbor hopping, as illustrated in Fig. 2(c). In this case, Avila's global theory can be applied to analytically characterize the localization properties of the dressed particles.

To elaborate the physics of this universal result, we consider the generic eigen-equation for the current spinful QP system that $H|\Psi\rangle = E|\Psi\rangle$, with $|\Psi\rangle = \sum_{j=1}^L (c_{j,\uparrow}^\dagger u_{j,\uparrow} + c_{j,\downarrow}^\dagger u_{j,\downarrow})|\text{vac}\rangle$, which is given by

$$\Pi_{j-1}^\dagger \vec{u}_{j-1} + \Pi_j \vec{u}_{j+1} + M_j \vec{u}_j = E \vec{u}_j \quad (11)$$

where $\vec{u}_j = (u_{j,\uparrow}, u_{j,\downarrow})^\top$ denotes the spinor for spin-1/2 particles. Under the constraint described in Eq. (10), the hopping coupling matrix takes one of the following fundamental forms: for spin-conserved processes, $\tilde{\Pi}_j \sim (\sigma_0 \pm \sigma_z)/2 = \Lambda_\pm$; for spin-flipped processes, $\tilde{\Pi}_j \sim (\sigma_x \pm i\sigma_y)/2 = \sigma_\pm$; or a combination of both processes. Such constraint reduces the otherwise complicated eigen-equation in Eq. (11) to an effective 1D spinless QP chain with nearest-neighbor hopping. Here, $\tilde{\Pi}_j$ represents the hopping coupling matrix after a local unitary transformation, and the transformed spinor is denoted by \vec{v}_j . We present the essential physics for the first two fundamental cases in the main text, and additional details for all three cases can be found in Appendix D.

For the spin-conserved constraint, $\tilde{\Pi}_j \sim t_j \Lambda_\pm$, the spin-up and spin-down particles can dress each other via

$$v_{j,\downarrow} = \frac{M_j^{21}}{E - M_j^{22}} v_{j,\uparrow}. \quad (12)$$

In this transformed basis, we denote $v_{j,\downarrow} = \psi_j$, and the original eigen-equation in Eq. (11) can be reduced to effective 1D chain with unchanged nearest-neighbor hopping, given by

$$t_{j-1} \psi_{j-1} + t_j \psi_{j+1} + V_j^{\text{eff}} \psi_j = E \psi_j, \quad (13)$$

where the effective energy-dependent on-site potential is

$$V_j^{\text{eff}} = M_j^{11} + \frac{M_j^{12} M_j^{21}}{E - M_j^{22}}. \quad (14)$$

Such on-site potential can serve as effective IDZs, which generates critical states in the system. By tailoring the on-site matrix, one can engineer an effective unbounded potential for the dressed particle, even when all couplings in the system are finite. This arises from resonant coupling between the system's energy E and the on-site modulation of the single species M_j^{22} , resulting in a divergent effective on-site potential. The divergence in the potential effectively partitions the 1D system into multiple subchains, manifesting IDZs in the hopping, and driving the delocalized eigenstates into critical states. Notably, this resonant coupling mechanism is generic, not limited to the exactly solvable regime, and can be extended to systems beyond the exactly solvable conditions.

For the spin-flipped constraint, $\tilde{\Pi}_j \sim t_j \sigma_\pm$, similarly, in the transformed basis

$$v_{j,\downarrow} = \frac{t_j v_{j+1,\uparrow} + M_j^{21} v_{j,\uparrow}}{E - M_j^{22}}, \quad (15)$$

the original eigen-equation is reduced to

$$t_{j-1}^{\text{eff}} \psi_{j-1} + t_j^{\text{eff}} \psi_{j+1} + V_j^{\text{eff}} \psi_j = E \psi_j, \quad (16)$$

with effective hopping coefficient and on-site potential

$$t_j^{\text{eff}} = \frac{t_j M_j^{12}}{E - M_j^{22}}, \quad V_j^{\text{eff}} = M_j^{11} + \frac{t_{j-1}^2}{E - M_{j-1}^{22}} + \frac{M_j^{12} M_j^{21}}{E - M_j^{22}}. \quad (17)$$

The effective hopping and on-site potentials in Eqs. (14) and (17) highlight the requirement for p_j^s and the off-diagonal elements of M_j to be either constant or purely quasiperiodic in order to preserve exact solvability, as outlined in Theorem III (Sec. III C). The effective eigen-equation for the dressed particles involves processes such as $M_j^{12} M_j^{21}$, $t_j M_j^{12}$, and t_{j-1}^2 . These terms maintain a single QP frequency modulation when p_j^s and off-diagonal elements of M_j are either constant or purely quasiperiodic. However, when these terms are a mixture of constant and QP components, such as in the form $[A + B \cos(2\pi\alpha j)]^2$, they lead to mixed frequency modulations, thereby breaking the exact solvability.

The effective hopping coefficient and on-site potential in Eq. (17) also explain the guiding principle from theorem II (Sec. III B), where critical states arise if the system possesses IDZs in the shared components of both coupling matrices. Specifically, for the hopping coupling matrix $\Pi_j \sim t\sigma_+$, the presence of IDZs in $M_j^{1,2}$, which couples to σ_x and (or) σ_y , ensures that the effective 1D system exhibits IDZs, hence leading to the emergence of critical states. This result is exemplified by the absence (or presence) of critical states in type-I (or type-II) QP mosaic models [19, 37]. For a unified characterization, we describe the both types of quasiperiodic mosaic models in the spin-1/2 QP framework, which can be written as (see more details in Appendix E)

$$H_M = \sum_j \lambda(c_{j+1}^\dagger \sigma_- c_j + \text{h.c.}) + \sum_j c_j^\dagger V_j^M c_j. \quad (18)$$

Here $c_j = (c_{j,\uparrow}, c_{j,\downarrow})^\top$ is the spinor for the annihilation operators, and λ is the uniform hopping strength. The onsite matrix V_j^M distinguishes the type-I and type-II mosaic lattices, respectively given by

$$V_j^{M,I} = 2V_0 V_j^d \Lambda_+ + \lambda \sigma_x, \quad (19)$$

and

$$V_j^{M,II} = 2t V_j^d (\sigma_0 + \sigma_x), \quad (20)$$

with V_0 and t being the strength of QP modulation of the on-site matrix for type-I and type-II mosaic models, respectively. In the type-I quasiperiodic mosaic model, there are no IDZs in the shared components, resulting in a spectrum composed solely of extended and localized states [19]. In contrast, for the type-II quasiperiodic mosaic model, IDZs appear on σ_x , which introduces energy-dependent quasiperiodic hopping and an unbounded on-site potential, thereby giving rise to rigorously defined critical states within the spectrum [37].

The universal results offer a powerful guidance to construct exactly solvable models hosting all types of localization physics. The effective hopping and onsite coupling terms [Eq. (14)-(17)] provide a framework for designing the microscopic details of these systems by controlling the energy and coupling between the internal degrees of freedom. For example, by designing the effective potential, one can induce or suppress critical states, as well as manipulate the localization length.

D. New exactly solvable mosaic models

With the universal results presented above, we put forward several new exactly solvable models derived from the type-II QP mosaic model [37] in Eq. (18) and Eq. (20) by removing the MEs. Through a combination of dual transformation, we can construct new nontrivial models, which demonstrate the applications of the above results, and investigate the phase diagram of the models

both analytically and numerically. We numerically solve the spectrum and employ the fractal dimension (FD) to phenomenologically characterize the localization properties of the eigenstates $|\Psi\rangle = \sum_{j=1}^L u_j a_j^\dagger |\text{vac}\rangle$, where $\text{FD} = -\lim_{L \rightarrow \infty} \ln \sum_{j=1}^L |u_j|^4 / \ln L$, with u_j being the wave function coefficients, L the system size. In 1D, the FD approaches 1 for extended states and 0 for localized states, while for critical states, $0 < \text{FD} < 1$. The FD quantifies the effective dimension experienced by an eigenstate: extended states uniformly spread across the system, yielding $\text{FD} = 1$. Localized states decay exponentially, effectively perceiving zero dimension, hence $\text{FD} = 0$. Critical states, however, exhibit self-similar wave function structures that span the entire system, resulting in an effective dimension between 0 and 1.

We begin with the type-II QP mosaic model [37] in Eq. (18) and Eq. (20), whose Hamiltonian is given by

$$H_{M-II} = \sum_j \lambda(c_{j+1}^\dagger \sigma_- c_j + \text{h.c.}) + 2t \sum_j V_j^d c_j^\dagger (\sigma_0 + \sigma_x) c_j, \quad (21)$$

where λ is the uniform hopping strengths and t is the strength of balanced QP potential and exchange coupling. The spectrum comprises critical (localized) states for the energies satisfy $E < |\lambda|$ ($E > |\lambda|$) [37]. Next, we construct new exactly solvable models that host pure critical and localized phases by eliminating the MEs, as outlined in theorem I (Sec. III A). This is accomplished by removing the spin-independent component of the onsite matrix of the type-II QP mosaic model. This results in a quasiperiodic spin-flipped (QPSF) model given by

$$H_{\text{QPSF}} = \sum_j \lambda(c_{j+1}^\dagger \sigma_- c_j + \text{h.c.}) + 2t \sum_j V_j^d c_j^\dagger \sigma_x c_j. \quad (22)$$

This model is exactly solvable, as the hopping coupling matrix satisfies $\det|\sigma_\pm| = 0$. Applying Avila's global theory, we find that the system is in the localized phase when QP spin-flipped process dominates $|t| > |\lambda|$, with the analytic localization length $\xi_l = 2/\log|V/t|$ for all eigenstates. In contrast, when $|t| < |\lambda|$, the system is in the critical phase. The numerical results, as shown in Fig. 3(a), are consistent with the analytical results, with the dashed line marking the phase transition at $\lambda = t$.

The physics can be understood as follows: In the limit $\lambda \rightarrow 0$, the QP on-site term localizes the system into dimmers with eigenenergies $E = \pm 2tV_j^d$. In this case, the energy difference between adjacent site fluctuates significantly, and turning on the uniform hopping λ only hybridize a few dimmers with close energies, giving a localized phase. Conversely, in the limit $t \rightarrow 0$, the uniform spin-flipped hopping creates degenerate dimers with flat band energies $E = \pm\lambda$. The degeneracy of these dimers is then lifted by the QP on-site term V_j^d , which hybridizes them drastically, leading to a delocalized phase. The delocalized states are guaranteed to be critical due to the IDZs in the effective hopping

$$t_j^{\text{eff}} = \lambda V_j^d / E. \quad (23)$$

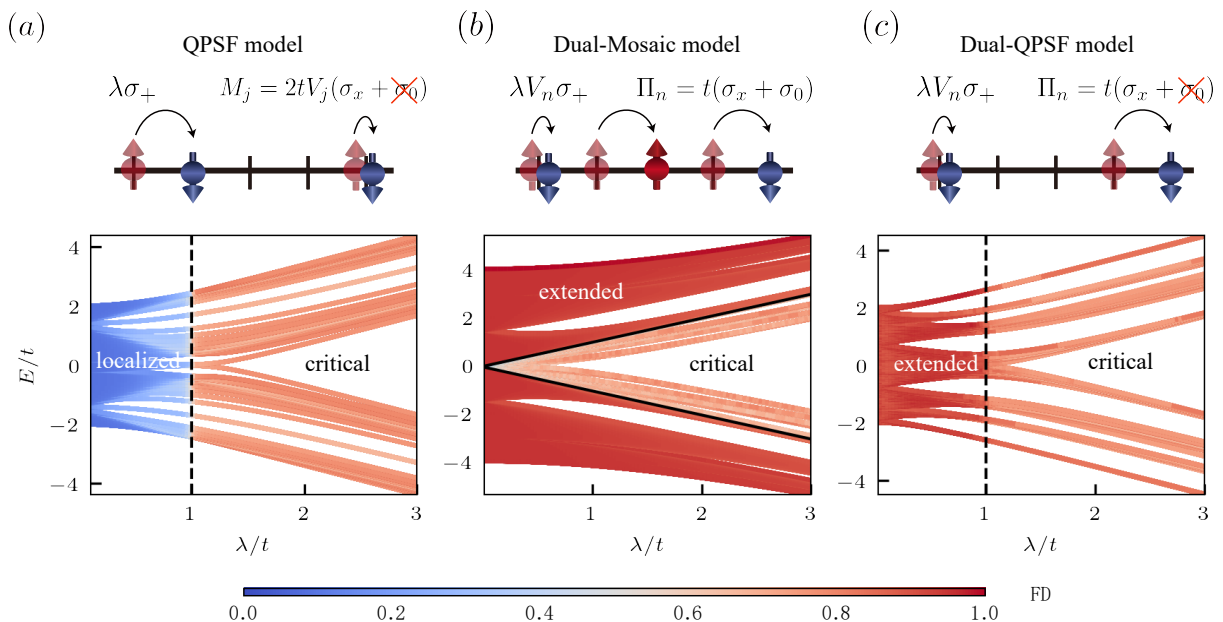


Figure 3. New exactly solvable models constructed using universal results and dual transformations. The fractal dimension (FD) as a function of energy E and hopping strengths λ/t . (a) The quasiperiodic spin-flipped (QPSF) model, derived by removing the σ_0 component of the type-II QP mosaic model, exhibits pure localized and critical phases. (b) The dual counterpart of the type-II QP mosaic model, featuring analytic mobility edges (MEs) that separate extended and critical states. The MEs occur at $E_c = \pm\lambda$ and are marked by solid lines. (c) The dual counterpart of the QPSF model, which is equivalent to removing the σ_0 component in the dual model from (b). The dual-QPSF model exhibits pure extended and critical phases, with the phase transition points $\lambda = t$ marked by dashed lines. The system size is $L = 2586$.

Furthermore, we can develop new models by performing dual transformations to the two aforementioned models, which exhibit mobility edges or phase transitions between critical and extended states. Applying the dual transformation to the type-II QP mosaic in Eq. (21) results in the following dual counterpart

$$\text{Dual}[H_{M-II}] = \sum_n t c_{n+1}^\dagger (\sigma_x + \sigma_0) c_n + \lambda c_n^\dagger V_n \sigma_+ c_n + \text{h.c.}, \quad (24)$$

with $V_n = \lambda \exp(i2\pi\alpha n)$. The model exhibits analytic MEs at $E_c = \pm\lambda$, with extended states for $E > |\lambda|$ and critical states for $E < |\lambda|$, as illustrated in Fig. 3(b). The absence of the localized orbitals can be understood as follows: under the local rotation $U = \exp(-i\pi\sigma_y/4)$, the coupling matrices of the dual model become

$$\tilde{T}_n = 2t\Lambda_+, \quad \tilde{M}_n = \lambda [\cos(2\pi\alpha n)\sigma_z + \sin(2\pi\alpha n)\sigma_y]. \quad (25)$$

In the limit $t \rightarrow 0$, the system yields two flat bands from the on-site matrix with energies $E = \pm\lambda$. The quantum states of the flat bands can be combined into either localized, extended, or critical states. The extended states and critical states are driven by the uniform hopping and the IDZs in the shared component, respectively.

Similarly, the dual QPSF model can be obtained by

$$\text{Dual}[H_{\text{QPSF}}] = \sum_n t c_{n+1}^\dagger \sigma_x c_n + \lambda c_n^\dagger V_n \sigma_+ c_n + \text{h.c.}, \quad (26)$$

with $V_n = \lambda \exp(i2\pi\alpha n)$, which is equivalent to removing spin-independent component from the previous dual model [Eq. (24)]. Through the duality transformation, this model exhibits a phase transition between pure critical and extended phases, with the critical phase for $|\lambda| > |t|$ and the extended phase for $|\lambda| < |t|$, with the correlation length given by $\xi_c = 2/\log|V/t|$. The numerical results agree with the analytic predictions as shown in Fig. 3(c). This demonstrates Theorem III in Sec. III C, which states that the model can be analytically characterized by investigating its dual counterpart.

IV. EXACTLY SOLVABLE MODELS FOR ALL FUNDAMENTAL LOCALIZATION PHASES

From the above subsection we can see that the universal results provide a powerful guidance to construct new exactly solvable models with nontrivial localization physics. In this section, we present the further in-depth study in developing the highly novel models with exact solutions, which enable a comprehensive and unified characterization of all the basic types of MEs and pure phases in quasiperiodic lattices. In particular, we propose two classes of exactly solvable models. The first is 1D spin-selective QP (SSQP) lattice model which is shown to host all basic types of MEs, and the second is the QP optical Raman lattice model which hosts all the seven fundamen-

tal localization phases. The seven fundamental phases are the three pure phases (extended, critical, and localized), three coexisting phases for any two of the three types of states, and one coexisting phase with all three types of states.

In the following, we first study the the exactly solvable models for all types of fundamental MEs. Then we show that the QP optical Raman lattice model can host all the seven fundamental localization phases.

A. The spin-selective QP lattice model for all fundamental MEs

The SSQP lattice model for spin-1/2 fermions includes several ingredients. First, the QP hopping or QP onsite potential of the model is considered only for fermions at one spin state, while fermions at another spin state are coupled through the uniform spin-flip transitions. Second, the GIZs are introduced to the hopping matrix Π_j or the shared component of M_j , leading to the emergence of the critical states. Third, the spin-independent coupling term is applied to break chiral symmetry, such that MEs emerge. The Hamiltonian is taken in a generic form

$$H = \sum_j \left[c_{j+1}^\dagger \left(t\Lambda_+ + \mu V_j^{\text{od}} \Lambda_- + \lambda_1 \sigma_x \right) c_j + \text{h.c.} \right] + \sum_j c_j^\dagger \left[(V_0 + 2V_B V_j^{\text{d}}) \Lambda_- + \lambda_0 \sigma_x \right] c_j. \quad (27)$$

We first consider the exactly solvable regime that hosts MEs separating critical and extended states, with its dual counterpart hosting MEs separating critical and localized states. In particular, we take the condition $t = V_0 = V_B = 0$ and $\lambda_0 = \lambda_1 = \lambda$. The SSQP model [Eq. (27)] has QP hopping only for the spin-down fermions, whereas the spin-up fermions are coupled through uniform spin-flip tunneling and on-site transitions. In this case, the coupling matrices reduce to

$$\Pi_j = \mu V_j^{\text{od}} \Lambda_- + \lambda \sigma_x, \quad M_j = \lambda \sigma_x. \quad (28)$$

Fig. 4(b) left subfigure shows the model exhibits MEs separating critical and extended states at $E_c = \pm \lambda^2/\mu$. For energies $E < |\lambda^2/\mu|$, the system exhibits extended states, while for energies $E > |\lambda^2/\mu|$, critical states are observed. These results can be derived analytically by investigating the dual counterpart, whose coupling matrix is degenerate $|\Pi_n| = 0$ (Sec. III B) and is given by

$$\Pi_n = \mu V_n^{\text{od}} \Lambda_-, \quad (29)$$

$$M_n = \lambda [\sigma_x + \cos(2\pi\alpha n) \sigma_x + \sin(2\pi\alpha n) \sigma_y].$$

By reducing the system to an effective 1D spinless model, the effective hopping and on-site potential are given by

$$t_n^{\text{eff}} = \mu V_n^{\text{od}}, \quad V_n^{\text{eff}} = \lambda^2 (2 + 2V_n^{\text{d}}) / E. \quad (30)$$

Neglecting the constant term in the potential, this effective model can be viewed as 1D extended Aubry-André (EAA) model [40, 41, 44] without uniform hopping, where the system is in the localized (critical) phase when the QP potential (QP hopping) dominates (see Appendix A for details). Therefore, the system is in the critical phase for $\mu > \lambda^2/|E|$ and in the localized phase for $\mu < \lambda^2/|E|$. The numerical results shown in Fig. 4(b) right subfigure are consistent with this analytic study. The MEs, $E_c = \pm \lambda^2/\mu$, separate the critical states for $|E| < \lambda^2/\mu$ from the localized states for $|E| > \lambda^2/\mu$. These results can also be obtained by applying Avila's global theory, yielding the LE

$$\gamma(E) = \frac{1}{2} \ln \left| \left| \lambda^2/\mu E \right| + \sqrt{(\lambda^2/\mu E)^2 - 1} \right|, \quad (31)$$

which not only provides the MEs, but also gives the localization length $\xi_l = \gamma^{-1}(E)$ for the localized states.

With the above results in the dual space, we can easily obtain the analytic characterization in the original space. Specifically, for $E < |\lambda^2/\mu|$, the eigenstate with energy E in real space is extended, with a correlation length $\xi_e = \gamma^{-1}(E)$, as localized states are transformed into extended states under the dual transformation. For $E > |\lambda^2/\mu|$, the eigenstate with energy E remains critical.

We further consider another more exotic exactly solvable regime that realizes all three basic types of MEs, namely the MEs separating extended from localized states, extended from critical states, and critical from localized states. This corresponds to $\mu = \lambda_1 = 0$, for which the QP onsite potential is applied solely to the spin-down fermions in the SSQP model. The spin-up fermions have a uniform hopping, and are coupled to spin-down states through the onsite spin-flip transitions. In this regime the coupling matrices simplify to

$$\Pi_j = t\Lambda_+, \quad M_j = (V_0 + 2V_B V_j^{\text{d}}) \Lambda_- + \lambda_0 \sigma_x. \quad (32)$$

The phase diagram in Fig. 4(c) reveals all three fundamental MEs resulting from the interplay between IDZs in shared components (σ_z, σ_0) and the broken chiral symmetry. When V_B/t is sufficiently large, the spectrum exhibits only critical and localized states, with MEs $E_c = \pm 2t$ separating the critical states ($|E| < 2t$) and the localized states ($|E| > 2t$). For intermediate V_B/t , extended orbitals also appear in the spectrum.

The underlying physics of the emergence of the three types of MEs can be achieved by by reducing the SSQP model in the current regime [Eq. (32)] to an effective 1D spinless model, where the effective energy-dependent on-site potential induced by IDZs in shared components plays a key role

$$t_j^{\text{eff}} = t, \quad V_j^{\text{eff}} = \lambda_0^2 / (E - V_0 - 2V_B V_j^{\text{d}}). \quad (33)$$

When $|E - V_0| \leq 2V_B$, the system exhibits an incommensurately distributed divergent potential, leading to the critical states. This explains why, when V_B/t is suffi-

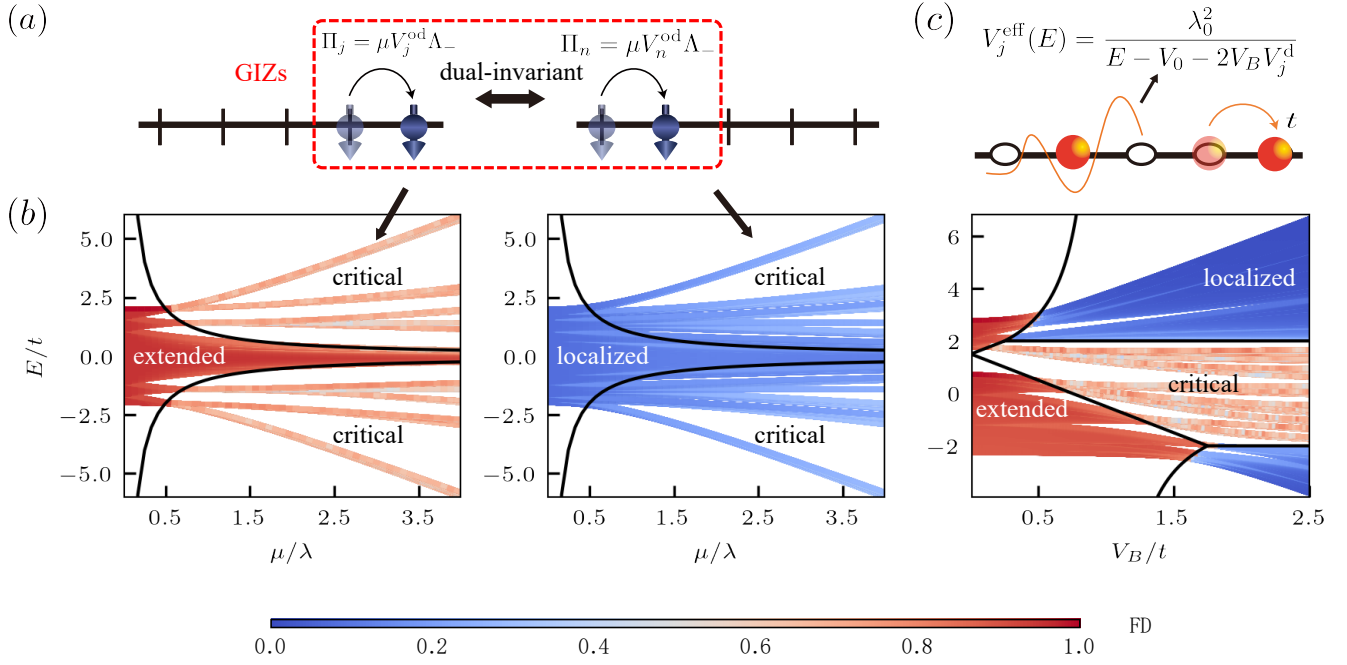


Figure 4. Generalized incommensurate zeros generated critical states. (a) The quasiperiodic spin-conserved hopping in this model gives rise to generalized incommensurate zeros (GIZs), which introduces critical orbitals in the system. (b) New exactly solvable model with generalized incommensurate zeros in matrix elements: Left panel: The model exhibits analytic mobility edges (MEs) at $E_c = \pm \lambda^2/\mu$, marked by the solid lines, which separate the extended states ($E < |\lambda^2/\mu|$) with fractal dimension (FD) approaching 1, and the rigorous critical states ($E > |\lambda^2/\mu|$) with FD approaching a value between 0 and 1. Right panel: The corresponding FD for the dual model. The MEs $E_c = \pm \lambda^2/\mu$ (solid lines) now separate the localized states ($E < |\lambda^2/\mu|$) and the rigorous critical states ($E > |\lambda^2/\mu|$). (c) Exactly solvable model hosting all MEs: Upper panel: The energy-dependent effective potential resulting from the incommensurately distributed zeros in the shared component, which now acts as the IDZs on the effective dressed particle. Lower panel: The FD of the eigenstates shown as a function of V_B/t and energy E/t , with $\lambda_0/t = 1$ and $V_0/t = 1.5$. The mobility edges are indicated by the solid lines. All systems have a size of $L = 2586$.

ciently large, the system exhibits only critical and localized states. In this regime, the analytic LE is

$$\gamma(E) = \ln \left| \frac{|E/t| + \sqrt{(E/t)^2 - 4}}{2} \right|, \quad (34)$$

with which the MEs reads $E_c = \pm 2t$. This result exemplifies a resonant coupling mechanism for critical states: when the onsite coupling is zero ($\lambda_0 = 0$), the two spin states decouple. The spin-down states produce a set of localized orbitals with energies $E_j = V_0 + 2V_B \cos(2\pi\alpha_j)$, while the spin-up states produce extended orbitals. Resonantly hybridizing these orbitals leads to divergent effective on-site potential, generating critical states.

When $|E - V_0| > 2V_B$, the effective potential is finite, giving extended and localized states. The LE can be analytically obtained as

$$\gamma(E) = \max \left\{ \ln \left| \frac{\chi_E + \sqrt{\chi_E^2 - \chi_B^2}}{|\chi_0| + \sqrt{\chi_0^2 - \chi_B^2}} \right|, 0 \right\}, \quad (35)$$

with $\chi_B = 2V_B/t$, $\chi_E = EV_B/t^2$ and $\chi_0 = (E - V_0)/t$. A finite $\gamma(E)$ gives the localized states with localization length $\xi_l = \gamma^{-1}(E)$, and $\gamma(E) = 0$ corresponds to the extended states.

Finally, by combining transition conditions for different effective potential and the corresponding LEs from Eq. (34) and Eq. (35), we determine the analytic MEs that separate extended, localized and critical states, as illustrated in Fig. 4(c) and summarized in Table I.

Conditions	Phases
$ E - V_0 > \max\{2V_B, E V_B\}$	Extended
$2V_B > \max\{ E - V_0 , E V_B\}$	Critical
$ E V_B > \max\{ E - V_0 , 2 V_B\}$	Localized

Table I. The criteria for the eigenstates with energies E to belong to one of the three phases: extended, critical, or localized, based on the relationship between the energy E , the on-site potential V_0 , and the quasiperiodic modulation strength V_B .

B. The model with the seven fundamental localization phases

We now show a highly novel result that the seven fundamental localization phases can be realized in the 1D QP optical Raman lattice model [47], as illustrated in

Fig. 5(a). This model is constructed by manipulating the IDZs in the shared components and the chiral symmetry. Specifically, in the presence of chiral symmetry, three distinct pure phases are obtained. Breaking chiral symmetry introduces MEs and four additional coexisting phases. The Hamiltonian is

$$H = \sum_j \left[c_{j+1}^\dagger (t_0 \sigma_z + i t_{so} \sigma_y) c_j + \text{h.c.} \right] + M_z \sum_j c_j^\dagger \left[\eta V_j^d \sigma_z + (1 - \eta) V_j^d \sigma_0 \right] c_j, \quad (36)$$

where t_0 and t_{so} denote spin-conserved and spin-flipped hopping coefficients, M_z is the strength of QP Zeeman potential, and η is the chiral parameter that controls the ratio of spin-dependent to spin-independent QP potentials, governing the extent of chiral symmetry breaking.

Fig. 5(b) illustrates the seven fundamental phases by varying the QP Zeeman potential M_z and the parameter η . These results are obtained by numerically diagonalizing the QP optical Raman lattice model in Eq.(36) with $t_{so} = 0.8t_0$. We first examine two limiting cases: exact chiral symmetry ($\eta = 1$) and complete chiral symmetry breaking ($\eta = 0$), followed by a discussion of the intermediate value of η . In the case of complete chiral symmetry breaking $\eta = 0$, corresponding to a purely spin-independent QP potential, the system exhibits extended and localized phases in the weak and strong quasiperiodic potential regimes, respectively. In this case, the transition energies remain outside the eigenstate spectrum, preserving the pure phases. For the intermediate value of η , a coexisting phase (L+E) emerges, with MEs separating extended and localized states. This result can be understood as follows: in the absence of spin-flipped hopping ($t_{so} = 0$), the model in Eq.(36) describes two decoupled spin-up and spin-down QP chains with opposite energy spectra, where each chain hosts either purely localized or extended phases. Turning on t_{so} couples the two chains, opening gaps within each and flattening the dispersion of original band states. This coupling localizes part of states in the moderate potential regime, leading to the formation of MEs. On the other hand, in the chiral symmetry limit $\eta = 1$, which corresponds to purely QP Zeeman potential, distinct phases appear in the weak, moderate, and strong field regimes, corresponding to pure extended, critical, and localized phases, respectively. These results are consistent with the predictions of Theorem I (Sec.III A) and previous studies [43, 47]. As indicated by theorem I and II, coexisting phases involving critical states (C+E, L+C, L+E+C) necessitate introducing generalized incommensurate zeros in matrix elements and breaking chiral symmetry. This corresponds to the presence of both spin-dependent and spin-independent QP potentials. Fig. 5(b) indicates that these phases occur for $\eta_c < \eta < 1$, with $\eta_c \approx 0.43$.

The emergence of the seven fundamental phases can be analytically predicted by combining the universal results and Avila's global theory. By applying Theorem III

in Sec. III C, the system is reduced to a spinless 1D QP chain with nearest-neighbor hopping when $\det |\Pi_j| = 0$, which occurs when $|t_0| = |t_{so}|$. We set $t_0 = t_{so}$ without losing generality. The system exhibits chiral symmetry at $\eta = 1$, where only pure critical and localized phases exist when $t_{so} = t_0$, and all three pure phases are present when $t_{so} \neq t_0$. Introducing a spin-independent quasiperiodic potential ($\eta \neq 1$) breaks chiral symmetry, leading to another exactly solvable point at $\eta = 1/2$, where MEs emerge within the original critical and localized phases for $t_{so} = t_0$, giving rise to the L+C phase. Further, various coexisting phases with combinations of the three types of quantum states emerge for $\eta < 1$ when $t_{so} \neq t_0$. Therefore, both numerical and analytical results confirm the existence of the seven fundamental localization phases, establishing this system as a universal quantum platform for exploration of localization physics.

In the following, we elaborate the entire phase diagram, starting from the high symmetry line $t_0 = t_{so}$, where the effective nearest-neighbor hopping is given by

$$t_j^{\text{eff}} = \frac{-2t_0\eta\Delta_j}{E - (1 - \eta)\Delta_j}, \quad (37)$$

with $\Delta_j = M_z V_j^d$. The energy-dependent effective on-site potential is given by

$$V_j^{\text{eff}} = \frac{4t_0^2}{E - (1 - \eta)\Delta_{j-1}} + \frac{E(1 - \eta)\Delta_j - (1 - 2\eta)\Delta_j^2}{E - (1 - \eta)\Delta_j}. \quad (38)$$

We first analyze the three limiting cases, $\eta = 0$, $\eta = 1$, and $\eta = 1/2$ while keeping $t_0 = t_{so}$, and then extend the discussion to cases where η deviates from these limits and $t_0 \neq t_{so}$, to explain the entire phase diagram.

1. Pure spin-independent quasiperiodic potential

For pure spin-independent limit of QP potential, where $\eta = 0$, the system exhibits only extended and localized states, with no critical states since IDZs in the shared component vanish. We first consider the high-symmetry case where $t_0 = t_{so}$, which leads to a vanishing effective hopping, leaving only the on-site potential

$$t_j^{\text{eff}} = 0, \quad V_j^{\text{eff}} = \frac{4t_0^2}{E - \Delta_{j-1}} + \Delta_j. \quad (39)$$

In this case, all eigenstates are localized as shown in Fig. 5(c1). The mechanism behind this can be understood as follows: when $M_z = 0$ (i.e., no QP Zeeman potential), the Hamiltonian [Eq. (36)] yields two flat bands, and any finite QP onsite potential M_z can fully localize all states. Deviating from the high-symmetry line $t_0 \neq t_{so}$ introduces next-nearest-neighbor (NNN) hopping $t_j^{\text{NN}} a_j^\dagger a_{j+2} + \text{h.c.}$, with coefficient

$$t_j^{\text{NN}} = \frac{t_+ t_-}{E - \Delta_{j+1}}, \quad (40)$$

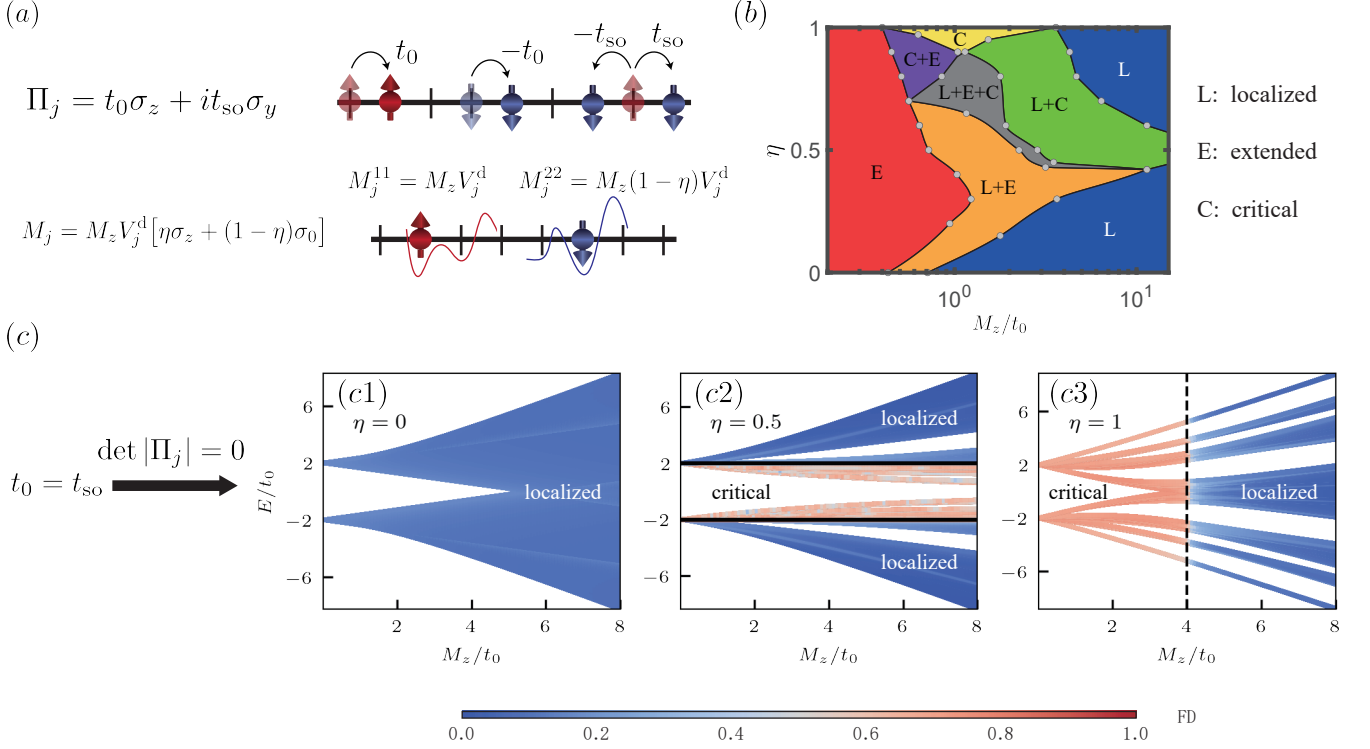


Figure 5. Seven fundamental phases of localization physics realized in 1D quasiperiodic (QP) optical Raman lattice. (a) Model Illustration: The hopping coupling matrix includes both spin-conserved and spin-flipped hopping terms, while the on-site matrix incorporates both spin-dependent quasiperiodic (QP) potential coupled to σ_z and spin-independent QP potential coupled to σ_0 . (b) Phase Diagram: The phase diagram, shown as a function of the QP Zeeman potential M_z and the chiral parameter η , reveals seven distinct phases. These consist of three pure phases: extended (E), localized (L), and critical (C), as indicated in the diagram. In addition, there are three coexisting two-phase regions: (L+E) for the coexistence of localized and extended states, (L+C) for localized and critical states, and (C+E) for critical and extended states. Moreover, a coexisting three-phase region (L+E+C) appears, where all three phases coexist. The phase diagram is obtained with the parameter set $t_{so} = 0.8t_0$. (c) Exact Solvable Points: (c1) When $\eta = 0$, the entire spectrum is localized. (c2) For $\eta = 0.5$, the spectrum splits into localized and critical states, with the mobility edges marked by solid lines at $E_c = \pm 2t_0$. States with $|E| < 2t_0$ are critical, while those with $|E| > 2t_0$ are localized. (c3) At $\eta = 1$, the system exhibits pure localized and critical phases, with the transition point marked by the dashed line at $M_z = 4t_0$. The system is in the localized (critical) phase when $M_z > 4t_0$ ($M_z < 4t_0$). The system size used in these calculations is $L = 2586$.

where $t_{\pm} = t_0 \pm t_{so}$. In this regime, nearest-neighbor hopping remains zero $t_j^{\text{eff}} = 0$, and on-site potential becomes

$$V_j^{\text{eff}} = \frac{t_+^2}{E - \Delta_{j-1}} + \frac{t_-^2}{E - \Delta_{j+1}} + \Delta_j. \quad (41)$$

The emergence of NNN hopping begins to destabilize localization, allowing for the appearance of delocalized states. Although the system is no longer analytically solvable for $t_0 \neq t_{so}$, the possible phases can still be determined. For sufficiently large (weak) M_z , the system always enters the localized (extended) phase. On the other hand, for intermediate M_z values, the chiral symmetry is explicitly broken by spin-independent QP modulation $M_z V_j^d \sigma_0$, leading to the emergence of mobility edges (MEs) between the extended and localized states. This accounts for extended, localized and L+E phases in Fig. 5(b) at $\eta = 0$, which extend to small η regime with $\eta < \eta_c \approx 0.43$.

2. Pure spin-dependent quasiperiodic potential

For pure spin-dependent QP potential, where $\eta = 1$, we begin by considering the scenario where $t_0 = t_{so}$, which yields the following effective hopping and on-site potential

$$t_j^{\text{eff}} = \frac{-2t_0\Delta_j}{E}, \quad V_j^{\text{eff}} = \frac{4t_0^2 + \Delta_j^2}{E}. \quad (42)$$

The corresponding Lyapunov exponent (LE) is given by

$$\gamma = \max \left\{ \frac{1}{2} \ln \left| \frac{M_z}{4t_0} \right|, 0 \right\}. \quad (43)$$

When $|M_z| > 4|t_0|$, the QP potential dominates, leading to a localized phase, where all states exhibit a localization length $\xi = \gamma^{-1}$. When $|M_z| < 4|t_0|$, the LE vanishes ($\gamma = 0$), and the system enters the critical phase. This

behavior is attributed to the IDZs in the hopping coefficients, consistent with the numerical calculations shown in Fig. 5(c3). No extended states are observed in this regime when $\eta = 1$ and $t_0 = t_{\text{so}}$ as expected.

We extend our analysis to the case where $t_0 \neq t_{\text{so}}$, which introduces modifications to the effective nearest-neighbor hopping and on-site potential due to the imbalance between t_0 and t_{so}

$$t_j^{\text{eff}} = \frac{t_- \Delta_{j+1} - t_+ \Delta_j}{E}, \quad V_j^{\text{eff}} = \frac{2t_0^2 + 2t_{\text{so}}^2 + \Delta_j^2}{E}, \quad (44)$$

and more importantly, such imbalance introduces an effective NNN hopping, with coefficient given by

$$t_j^{\text{NN}} = t_+ t_- / E. \quad (45)$$

This NNN hopping, induced by the imbalance between t_0 and t_{so} , gives rise to extended orbitals within the phase diagram. When the imbalance $|t_0 - t_{\text{so}}|$ is small relative to M_z , the critical states, generated by zeros in the hopping terms, remain dressed by the NNN hopping t_j^{NN} , preserving the critical phase. However, as the imbalance increases and t_j^{NN} dominates, the critical states transition into extended states [58].

The system exhibits the chiral symmetry at $\eta = 1$, leading to the vanishing MEs and the presence of only three pure phases: localized, extended, and critical. The global theory does not strictly apply here, however, since the system has no mobility edges, the phase boundaries can be determined by analyzing the typical eigenstates. For example, by considering the zero-energy states $E = 0$, the eigen-equation Eq. (36) for spin-up (spin-down) states ψ_j (φ_j) becomes

$$-t_0(\psi_{j+1} + \psi_{j-1}) - t_{\text{so}}(\psi_{j+1} - \psi_{j-1}) + \Delta_j \psi_j = 0, \quad (46)$$

with the φ obtained by replacing $t_{\text{so}} \rightarrow -t_{\text{so}}$. The above equation can be expressed in the form of transfer matrix as $(\psi_{j+1}, \psi_j)^\top = A_j(\psi_j, \psi_{j-1})^\top$, with A_j being

$$A_j = \begin{pmatrix} \Delta_j/t_+ & -t_-/t_+ \\ 1 & 0 \end{pmatrix}, \quad (47)$$

with an analogous form for spin-down states. In the pure spin-dependent limit ($\eta = 1$), the delocalized phase is topological while the localized phase is topologically trivial [47]. The phase boundary between the critical and localized phases can thus be determined by the topological transition. If both eigenvalues of the transfer matrix $A = \prod_{j=1}^L A_j$ are either less than 1 or greater than 1, the system is topological, and the ψ zero mode is localized at one end of the chain. Assuming $t_0 > 0$ and $t_{\text{so}} > 0$, then the two eigenvalues of A satisfy $|\lambda_1 \lambda_2| < 1$, the topological nature is dictated by the larger eigenvalue $|\lambda_2|$. After performing a standard similarity transformation [111, 112] or applying the global theory, we find the localized-to-critical transition point is given by $|M_z/2t_+| = 1$. By applying the same reasoning to the

transfer matrix in the dual space, the phase boundary between localized and critical phases in the dual space is $|M_z/2t_-| = 1$, corresponding to the transition between extended and critical phases in the original space. Therefore, for $\eta = 1$ and $t_0 \neq t_{\text{so}}$, the system exhibits three distinct pure phases as summarized in Table. II.

Conditions	Phases
$M_z < 2 t_- $	Extended
$2 t_- < M_z < 2 t_+ $	Critical
$M_z > 2 t_+ $	Localized

Table II. The criteria for the phases of 1D QP optical Raman lattice model at $\eta = 1$, based on the relationship between the QP Zeeman potential M_z and the imbalanced hopping $t_{\pm} = t_0 \pm t_{\text{so}}$.

When chiral parameter η deviates from $\eta = 1$, the chiral symmetry is broken and MEs appear. This leads to the emergence of the C+E phase, which interpolates between the pure critical and extended phases, and the L+C phase, which interpolates between the pure localized and critical phases, as shown in Fig. 5(b). Furthermore, as the chiral parameter η is further deviated from 1, the L+E+C phase emerges, interpolating between the C+E and L+E phases.

3. Balanced quasiperiodic potential

For balanced QP potential with $\eta = 1/2$, the energy-dependent effective nearest-neighbor hopping and on-site potential are given by

$$t_j^{\text{eff}} = \frac{-2t_0 \Delta_{j-1}}{2E - \Delta_{j-1}}, \quad V_j^{\text{eff}} = \frac{8t_0^2}{2E - \Delta_{j-1}} + \frac{E \Delta_j}{2E - \Delta_j}. \quad (48)$$

Applying Avila's theory, the LE for the system is

$$\gamma(E) = \max \left\{ \frac{1}{2} \ln \left| |E/2t_0| + \sqrt{E^2/4t_0^2 - 1} \right|, 0 \right\}. \quad (49)$$

The states with energy $|E| > 2|t_0|$ are localized, with localization length $\xi(E) = \gamma^{-1}(E)$. The states are critical when $|E| < 2|t_0|$, as the $\gamma(E) = 0$ and the hopping terms have IDZs. Consequently, $E = \pm 2t_0$ are critical energies separating localized and critical states, indicating the presence of MEs as shown in Fig. 5(c2). Thus, for $\eta = 1/2$ and $t_0 = t_{\text{so}}$, the system is in L+C phase. We extend this analysis to the case where $t_0 \neq t_{\text{so}}$, introducing an effective NNN hopping term given by

$$t_j^{\text{NN}} = \frac{-2t_+ t_-}{2E - \Delta_{j+1}}. \quad (50)$$

Similarly, the imbalance between t_0 and t_{so} generates extended orbitals within the spectrum, while critical states still exist when the NNN hopping t_j^{NN} is small relative to M_z . The combination of extended orbitals and the

L+C phase results in pure extended, L+E, and L+E+C phases. Similar phase transitions also occur when η deviates from $\eta = 1/2$. This analysis clarifies the origin of the L+C phase at the exactly solvable point $\eta = 1/2$ and $t_0 = t_{so}$, and demonstrates how the related phases, extended, critical, L+E, and L+E+C phases, emerge near $\eta = 1/2$, as depicted in Fig. 5(b).

C. Unified picture for the seven fundamental localization phases

We highlight the mapping relation between the present 1D QP optical Raman lattice model in Eq. (36) and the type-II QP mosaic model [37] in Eq. (21), with slightly modified on-site potential, given by

$$H_M = \sum_j \lambda (c_{j+1}^\dagger \sigma_- c_j + \text{h.c.}) + \sum_j V_j^d c_j^\dagger (2V_0 \sigma_0 + 2t \sigma_x) c_j. \quad (51)$$

Here, V_0 is the strength of the on-site potential. At the high symmetry line $V_0 = t$, the model Eq. (51) reduces to the origin one in Eq. (36), with analytic MEs between critical and localized states as discussed in Sec. III D. This mapping deepens our understanding for the entire phase diagram in Fig. 5(b).

The QP optical lattice model at $t_0 = t_{so}$ can be mapped to the type-II QP mosaic model [Eq. (51)] followed by a local rotation $U = \exp(-i\pi\sigma_y/4)$, with the coefficients between two models are related by the following substitution rule

$$\lambda \leftrightarrow 2t_0, \quad (52)$$

$$2t \leftrightarrow \eta M_z, \quad (53)$$

$$2V_0 \leftrightarrow (1 - \eta) M_z. \quad (54)$$

The pure spin-dependent QP potential limit ($\eta = 1$) of QP optical Raman lattice model corresponds to the type-II QP mosaic model in the limit $V_0 = 0$. In this scenario, both models are exactly solvable, exhibiting localized and critical phases. Specifically, the type-II QP mosaic model is in the localized phase when $|t| > |\lambda|$ and in the critical phase when $|t| < |\lambda|$ [Fig. 3(a)]. This is consistent with the QP optical Raman lattice model, where the localized phase occurs when $M_z > 4t_0$ and the critical phase when $M_z < 4t_0$ [Fig. 5(c3)].

Reducing the chiral parameter η from 1 to 1/2 corresponds to turning on the on-site potential V_0 in the type-II QP mosaic model, transitioning from $V_0 = 0$ to $V_0 = t$. Breaking the chiral symmetry of both models, introducing the MEs between localized and critical states, leading to the L+C phase. As the on-site potential increases towards the high-symmetry line $V_0 = t$, or when the QP optical Raman lattice model reaches $\eta = 1/2$, the system becomes analytically solvable again. The type-II QP mosaic model exhibits analytic MEs $E = \pm\lambda$ separating the localized and critical states [37], which corresponds to the MEs $E = \pm 2t_0$ in the QP optical Raman lattice model.

Further introducing the imbalance between t_0 and t_{so} leads to the emergence of extended phases and associated MEs. And this will lead to the long-range hopping terms when reduced the system into the spinless QP chain, introducing extended orbital into the spectrum of the type-II QP mosaic model. Thus, this mapping, combined with the imbalance between t_0 and t_{so} , accounts for the generation of the seven phases in the phase diagram.

V. SCHEMES FOR EXPERIMENTAL REALIZATION

In this section, we propose experimental schemes for realizing the SSQP on-site model [Eq. (32)] and QP optical Raman lattice model [Eq. (36)]. These schemes utilize ultracold alkali atoms, which are ideal candidates due to their large fine-structure energy splitting and moderate natural linewidth. These properties facilitate efficient Raman coupling and spin-dependent potentials, even when the laser frequency is far detuned from the D_1 and D_2 lines [113–115], making ultracold alkali atoms well-suited for implementing the QP lattice.

We first propose the scheme for the SSQP on-site model in Eq. (32) supporting all three basic MEs, as illustrated in Fig. 6(a-b), whose Hamiltonian is

$$H = \left[\frac{p_z^2}{2m} + \mathcal{V}_s(z) \right] \otimes \sigma_0 - \mathcal{V}_p(z) \Lambda_- + M_0 \sigma_x, \quad (55)$$

where the first term represents the kinetic energy. $\mathcal{V}_p(z) = V_p \cos(k_p z + \phi_p)$ is a deep spin-dependent primary lattice that freezes the spin-conserved hopping for spin-down atoms. The different terms in Eq. (32) can be realized as follows. The uniform spin-conserved hopping $\Pi_j = t \Lambda_+$ for spin-up atoms can be obtained by

$$t = - \int dz w_{s,\uparrow}^*(z) [p_z^2/2m + \mathcal{V}_s(z)] w_{s,\uparrow}(z - a_s), \quad (56)$$

where $w_{s,\uparrow}(z)$ is the Wannier function of the secondary lattice generated by spin-independent potential $\mathcal{V}_s(z) = V_s \cos(k_s z + \phi_s)$, with $a_s = \pi/k_s$ being the lattice constant. The potential $\mathcal{V}_s(z)$ is incommensurate with the potential $\mathcal{V}_p(z)$ for spin-down atoms, leading to the QP potential $M_j = 2V_B V_j^d \Lambda_-$ for spin-down atoms

$$\begin{aligned} 2V_B V_j^d &= \int dz \mathcal{V}_s(z) |w_{s,\downarrow}(z - ja_p)|^2 \\ &= 2V_B \cos(2\pi\alpha j + \phi_s), \end{aligned} \quad (57)$$

where $\alpha = k_s/k_p$, and $2V_B \equiv \int dz V_s \cos(k_s z) |w_{s,\downarrow}(z)|^2$. The Wannier function $w_{s,\downarrow}(z)$ is determined by the primary lattice, with the lattice constant $a_p = \pi/k_p$. Finally, the on-site spin-flipped term $M_j = \lambda_0 \sigma_x$ can be induced via $M_0 \sigma_x$ in Eq. (55).

The proposed Hamiltonian in Eq. (55) can be realized based on QP optical Raman lattice, as outlined below. The detailed implementation can be found in Appendix F. To facilitate the description, we perform a unitary transformation, such that $\sigma_z \rightarrow \sigma_x$ and $\sigma_x \rightarrow -\sigma_z$.

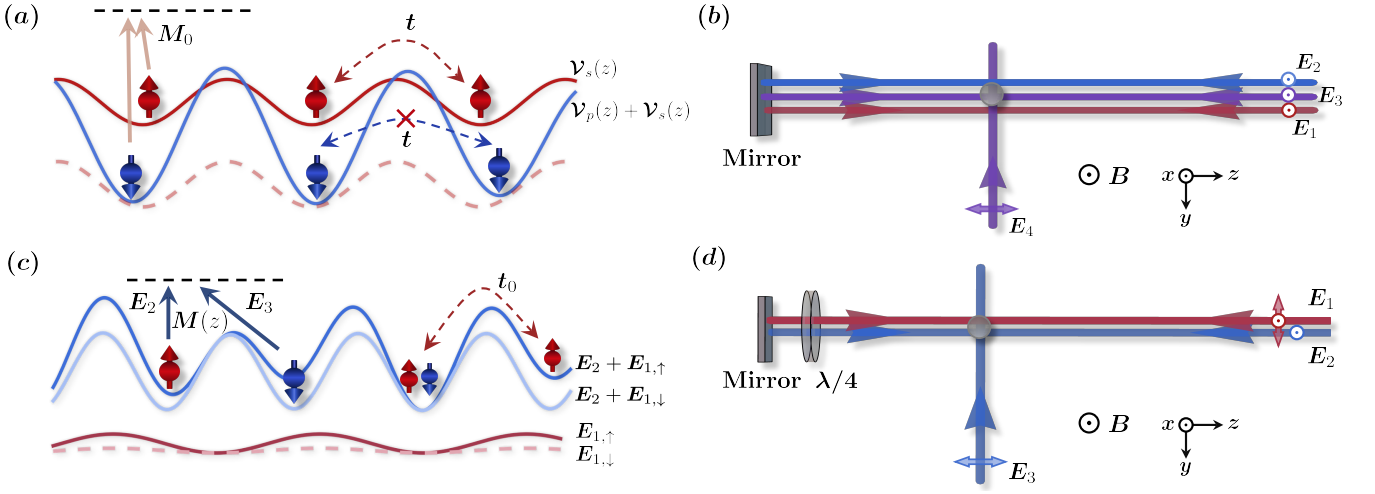


Figure 6. Experimental realization schemes. (a)-(b) Implementation of the model supporting all fundamental mobility edges (MEs) (a) The spin-conserved hopping for spin-down atoms is suppressed by a spin-dependent deep primary potential $\mathcal{V}_p(z)$ (blue solid line), while spin-up atoms undergo hopping in a secondary potential $\mathcal{V}_s(z)$ (red solid line). The on-site potential for spin-down atoms (red dashed line) is realized by the combination of $\mathcal{V}_p(z)$ and $\mathcal{V}_s(z)$, which are incommensurate with each other. The on-site spin-flipped process is introduced via an overall coupling M_0 . (b) Schematic of the experimental setup. The spin-dependent potential $\mathcal{V}_p(z)$ is formed by the combination of \mathbf{E}_2 and \mathbf{E}_3 with the traveling wave \mathbf{E}_4 , while the spin-independent secondary potential $\mathcal{V}_s(z)$ is generated by \mathbf{E}_1 , affecting both spin states. (c)-(d) Realization of the quasiperiodic optical Raman lattice model. (c) The spin-conserved hopping t_0 is induced by the primary lattice $\mathcal{V}_p(z)$, and the spin-flipped hopping t_{so} is induced by the Raman potential $\mathcal{M}(z)$. The quasiperiodic Zeeman potential is realized by the secondary lattice $\mathcal{V}_s(z)$. (d) Schematic of the setup. A standing wave \mathbf{E}_1 , combined with the blue-detuned spin-independent primary lattice generated by \mathbf{E}_2 , creates the spin-dependent Zeeman potential. A traveling wave \mathbf{E}_3 generates the Raman potential in combination with \mathbf{E}_2 .

The kinetic term and spin-independent potential $\mathcal{V}_s(z)$ remain unchanged and can be generated using the standing wave \mathbf{E}_1 . The rotated spin-dependent potential $\mathcal{V}_p(z)(\sigma_0 - \sigma_x)/2$ can be realized using a standing waves \mathbf{E}_2 and \mathbf{E}_3 along with a traveling wave \mathbf{E}_4 . Finally, the $M_0\sigma_z$ term arises from the two-photon detuning of the Raman coupling. After performing the inverse unitary transformation, we reach the Hamiltonian in Eq. (55). More details can be found in Appendix. F, where ^{87}Rb atoms are used as an example.

We then propose the scheme for the model supporting all seven fundamental phases [Eq. (36)] based on the QP optical Raman lattice [Fig. 6(c,d)], which has been successfully employed for the realization of synthetic gauge fields and the exploration of topological phases with ultracold atoms [88–96]. The Hamiltonian is given by

$$H = \left[\frac{p_z^2}{2m} + \mathcal{V}_p(z) + (1 - \eta)\mathcal{V}_s(z) \right] \otimes \sigma_0 + \mathcal{M}(z)\sigma_x + \eta\mathcal{V}_s(z)\sigma_z. \quad (58)$$

The different terms in Eq. (36) can be realized accordingly. The uniform hopping coupling $\Pi_j = t_0\sigma_z + it_{so}\sigma_y$ arises from the tunneling of the Wannier function of the primary lattice, where

$$t_0 = - \int dz w_s^*(z) [p_z^2/2m + \mathcal{V}_p(z)] w_s(z - a_0/2) \quad (59)$$

with $p_z^2/2m$ being the kinetic energy along the lattice direction z , a_0 the primary lattice constant, and $\mathcal{V}_p(z) = V_p \cos^2(k_p z)$ the spin-independent primary lattice realized by a blue-detuned standing wave \mathbf{E}_2 . The t_{so} is generated by the Raman potential

$$t_{so} = \int dz w_s^*(z) \mathcal{M}(z) w_s(z - a_0/2), \quad (60)$$

where $\mathcal{M}(z) = M_0 \cos(k_p z)$ represents the Raman potential formed by the intersection of x -polarized \mathbf{E}_2 and z -polarized traveling wave \mathbf{E}_3 , generating the spin-flipped hopping. The QP on-site matrix element is realized by the spin-dependent secondary lattice, which is given by

$$M_z V_j = \int dz \mathcal{V}_s(z) |w_s(z - ja_0)|^2 = V_s \cos(2\pi\alpha j + 2\phi_s), \quad (61)$$

where the QP parameter $\alpha = k_s/k_p$, and $\mathcal{V}_s(z) = V_s \cos^2(k_s z + \phi_s)$ is the spin-dependent secondary lattice generated by the composite standing wave \mathbf{E}_1 , formed by two counter-propagating beams with mutually perpendicular polarization along the x and y axes. The chiral parameter η is tuned by adjusting the power ratio of the two different polarizations of beam \mathbf{E}_1 . The spin-dependent term $\eta\mathcal{V}_s(z)\sigma_z$ from vector optical shift is induced by the y -polarization, while the spin-independent term $(1 - \eta)\mathcal{V}_s(z)\sigma_0$ is mainly contributed from the scalar components of both the x - and y -polarizations.

VI. CONCLUSION AND OUTLOOK

We have proposed a generic spin-1/2 quasiperiodic (QP) system that unifies the existing important 1D QP models, some of which requiring an extra Majorana representation, and established a unified framework for all fundamental localization phases in quasiperiodic systems. The framework is built on three universal results. First, we showed with renormalization group method the criteria for obtaining the pure phases, namely when the system has no mobility edges. Second, we uncovered a new universal mechanism for the emergence of critical states, as characterized by the generalized incommensurate zeros in matrix elements that remain invariant under the dual transformation and introduce critical orbitals into the system. Third, we identified the condition for the exact solvability of QP systems from local constraint, which also provides the mechanism to realize effective unbounded on-site potential in spinful QP chains. These results establish a profound unified theory for all fundamental localization phases in quasiperiodic systems, and offer the key insights for constructing their exactly solvable models. In particular, we proposed the novel spin-selective QP lattice model and QP optical Raman lattice model, in which we predict all basic types of mobility edges (MEs) and all the seven fundamental phases in Anderson localization physics, respectively, which have not been achieved anywhere else. Finally, we proposed experimentally feasible schemes to realize the theoretical predictions in optical Raman lattice.

This work enables a broad exploration and exact characterization of the fundamental quantum phases in Anderson localization and opens up intriguing topics for the future study. For example, while the present study is focused on the spin-1/2 QP systems, it is natural to extend the current study to the QP systems with larger spins, e.g. to the 1D $SU(N)$ QP chain with N larger than 2. Generalizing the mechanism of IDZs in matrix elements for critical states to the $SU(N)$ systems is of great interests to obtain the rigorous critical states in generic QP systems. The exact characterization of the distinct quantum phases in such $SU(N)$ QP system could potentially be connected to the exactly solvable QP mosaic models [19, 37] with large unit cells, and deserves particular future efforts. On the other hand, extending the present results to higher dimensions is another important issue for the future study.

Moreover, the newly proposed exactly solvable models in this work, which host various MEs, can further be implemented in the many-body regime. The different types of the MEs in this work, including the traditional ME separating localized and extended states, and the novel MEs involving critical states, can be considered to study the interplay between many-body localization, ergodic and many-body critical phases. The exact solvability of the model, which allows for the analytic characterization of the whole non-interacting spectrum, serves as an analytic platform to study the interplays among them.

ACKNOWLEDGMENTS

This work was supported by National Key Research and Development Program of China (Grants No. 2021YFA1400900, No. 2022YFA1405800 and No. 2020YFA0713300), the National Natural Science Foundation of China (Grants No. 12425401, No. 12261160368 and No. 12401208), the Innovation Program for Quantum Science and Technology (Grant No. 2021ZD0302000), the Shanghai Municipal Science and Technology Major Project (Grant No. 2019SHZDZX01), the Natural Science Foundation of Jiangsu Province (Grant No. BK20241431), the Nankai Zhide Foundation, and by the Fundamental Research Funds for the Central Universities (Grant No. 100-63253099).

Appendix A: 1D spinless QP model

In this section, we show that the 1D spinless QP model with nearest-neighbor hopping can also be unified within the spinful QP framework, under the Majorana representation. For a generic 1D spinless QP chain model, the tight binding Hamiltonian is given by

$$H = t_j \sum_j (c_j^\dagger c_{j+1} + \text{h.c.}) + \sum_j V_j c_j^\dagger c_j. \quad (\text{A1})$$

The t_j and V_j are the hopping coefficients and on-site potential, respectively. Such 1D spinless QP chain can be rewritten into the spinful QP chain by introducing the Majorana representation

$$c_j = \frac{1}{2}(\gamma_{B,j} + i\gamma_{A,j}), \quad c_j^\dagger = \frac{1}{2}(\gamma_{B,j} - i\gamma_{A,j}), \quad (\text{A2})$$

with $\gamma_{\sigma,j} = \gamma_{\sigma,j}^\dagger$ and $\{\gamma_{\sigma,j}, \gamma_{\sigma',j'}\} = 2\delta_{\sigma\sigma'}\delta_{jj'}$. In this basis, the Hamiltonian in Eq. A1 becomes

$$H = \frac{t_j}{2} \sum_j (i\gamma_{B,j}\gamma_{A,j+1} + i\gamma_{B,j+1}\gamma_{A,j}) + \sum_j \frac{V_j}{2} (1 + i\gamma_{B,j}\gamma_{A,j}). \quad (\text{A3})$$

One can neglect the last summation, which leads to a constant, then the generic Hamiltonian is unified within our 1D spinful formalism, with the hopping coupling matrix and the on-site matrix given by

$$\Pi_j = \frac{t_j}{4}\sigma_y, \quad M_j = \frac{V_j}{4}\sigma_y. \quad (\text{A4})$$

One characteristic is that both hopping coupling and on-site matrix share the same Pauli component σ_y , which is a hallmark of the spinless QP model rewritten in the spinful QP framework. This formalism unifies all the important 1D spinless QP model in this context, including the AA model [6], the extended AA (EAA) model [40, 41, 44], the

Models	t_j	V_j
AA model	t	$2V_0V_j^d$
EAA model	$(t + \mu)V_j^{\text{od}}$	$2V_0V_j^d$
GAA model	t	$2V_0V_j^d/(1 - aV_j^d)$

Table III. The parameters of different 1D spinless QP model

generalized AA (GAA) model [12], or the GPD model in some context. These are summarized in the table. III.

The conditions for the different states of the AA, EAA and GAA models are summarized in Table IV.

	Extended	Critical	Localized
AA	$t > V_0$	$t = V_0$	$t < V_0$
EAA	$t > \max\{\mu, V_0\}$	$\mu > \max\{t, V_0\}$	$V_0 > \max\{t, \mu\}$
GAA	$aE < 2(t - V_0)$	$aE = 2(t - V_0)$	$aE > 2(t - V_0)$

Table IV. The criteria for different states of AA, EAA and GAA models. Here E is the eigenenergies of the system. Without loss of generality, we assume of the hopping and on-site coefficients are positive.

Appendix B: Proof of criteria for the pure phases without MEs

In this section, we provide the detail of the proof of the criteria for the system exhibits pure phase and exhibits no mobility edges (MEs), as discussed in the main text, using the renormalization group technique.

Under the commensurate approximation of the irrational parameter, the system displays periodic structure and exhibit band dispersion. And the characteristic polynomial is given by the determinant $P^{(n)}(E; \kappa_x, \kappa_y) = |\mathcal{H}^{(n)} - E|$, which can be expanded over the principle dispersion

$$\begin{aligned}
P^{(n)}(E; \kappa_x, \kappa_y) &= t_R^{(n)} \cos(\kappa_x + \kappa_x^0) + V_R^{(n)} \cos(\kappa_y + \kappa_y^0) \\
&+ \mu_R^{(n)} \cos(\kappa_x + \tilde{\kappa}_x^0) \cos(\kappa_y + \tilde{\kappa}_y^0) \\
&+ \epsilon_R^{(n)}(E, \varphi, \kappa) + T_R^{(n)}(E). \quad (\text{B1})
\end{aligned}$$

The system exhibits pure phases without MEs correspond to the case that, the coefficients associated with the relevant dispersions are energy independent. In the presence of the commensurate approximation, then the band dispersion is periodic with respect to both $\kappa_x = Lk_x$ and $\kappa_y = Lk_y$. Here, k_x is the twisted momentum attached to the hopping coupling matrix $\Pi_j \rightarrow \Pi_j e^{ik_x}$ and k_y is the phase offset in the QP modulation V_j^d and V_j^{od} .

Since $P(E)$ has only real roots as H is Hermitian, so the dispersion and $P(E; \kappa_x, \kappa_y)$ shares similar periodicity, thus $P(E; \varphi, \kappa)$ is also periodic with respect to $\kappa_x = Lk_x$ and $\kappa_y = Lk_y$.

As indicated in the main text, we first diagonalize the on-site matrix M_j as $M_j = m_j^z \sigma_z + m_j^0 \sigma_0$, and the resulted hopping coupling matrix is still in the form $\Pi_j = \sum_s p_j^s \sigma_s$, with s being $s = \{0, x, y, z\}$. For the criteria that the coefficients of hopping coupling matrix satisfy

$$p_j^x/p_j^y = \text{Const.} \in \mathbb{R}, \quad (\text{B2})$$

and both coupling matrices exclude σ_0 , namely

$$\Pi_j = p_j^x \sigma_x + p_j^y \sigma_y + p_j^z \sigma_z, \quad M_j = m_j^z \sigma_z. \quad (\text{B3})$$

We can first simplify model by denoting $m_j^z \equiv m_j$ and

$$p_j^x = p_j^\perp \cos \theta, \quad p_j^y = p_j^\perp \sin \theta, \quad (\text{B4})$$

with $p_j^\perp = \sqrt{|p_j^x|^2 + |p_j^y|^2}$ and $\tan \theta = p_j^x/p_j^y$. Then the system can be rewritten in a more compact form by a unitary transformation

$$U(z, \theta) = \begin{pmatrix} e^{i\theta} & 0 \\ 0 & e^{-i\theta} \end{pmatrix}, \quad (\text{B5})$$

then the system becomes

$$\Pi'_{j-1} \vec{v}_{j-1} + \Pi_j^\dagger \vec{v}_{j+1} + M_j \vec{v}_j = E \vec{v}_j, \quad (\text{B6})$$

with the transformed hopping coupling matrix $\Pi'_j = U(z, \theta/2) \Pi_j U^\dagger(z, \theta/2)$ being

$$\Pi'_j = p_j^\perp \sigma_x + p_j^z \sigma_z, \quad (\text{B7})$$

and $\vec{v}_j = U(z, \theta) \vec{u}_j = \begin{pmatrix} v_{j\uparrow} & v_{j\downarrow} \end{pmatrix}^\top$.

Before proving the absence of the MEs when satisfying the criteria, we first identify the chiral symmetry of the system under this condition, which is highly related to the disappearance of the MEs. We notice that under the unitary operator $\mathcal{O} = \sigma_y$, both coupling matrices change sign, i.e.,

$$\mathcal{O} \Pi'_j \mathcal{O}^\dagger = -\Pi'_j, \quad \mathcal{O} M_j \mathcal{O}^\dagger = -M_j. \quad (\text{B8})$$

Therefore both \vec{v}_j and $\mathcal{O} \vec{v}_j$ are the eigenstate of the system, with the corresponding energies come in pair as $(E, -E)$.

With this properties, we proceed to calculate the characteristic polynomial $P(E)$. We first consider the eigen-

equation $H|v\rangle = E|v\rangle$ under the twisted boundary condition

$$\begin{aligned} e^{ik_x}(p_{j-1}^z v_{j-1\uparrow} + p_{j-1}^\perp v_{j-1\downarrow}) + e^{-ik_x}(p_j^{z*} v_{j+1\uparrow} + p_j^{\perp*} v_{j+1\downarrow}) + m_j v_{j\uparrow} &= E v_{j\uparrow}, \\ e^{ik_x}(p_{j-1}^\perp v_{j-1\uparrow} - p_{j-1}^z v_{j-1\downarrow}) + e^{-ik_x}(p_j^{\perp*} v_{j+1\uparrow} - p_j^{z*} v_{j+1\downarrow}) - m_j v_{j\downarrow} &= E v_{j\downarrow}, \end{aligned} \quad (\text{B9})$$

then we locally rotate the bases as $\psi_j^\pm = v_{j\uparrow} \pm i v_{j\downarrow}$, and we can rewrite the eigen-equation as

$$\begin{aligned} e^{ik_x}(p_{j-1}^z + i p_{j-1}^\perp) \psi_{j-1}^- + e^{-ik_x}(p_j^{z*} + i p_j^{\perp*}) \psi_{j+1}^- + m_j \psi_j^- &= E \psi_j^- \\ e^{ik_x}(p_{j-1}^\perp - i p_{j-1}^z) \psi_{j-1}^+ + e^{-ik_x}(p_j^{\perp*} - i p_j^{z*}) \psi_{j+1}^+ + m_j \psi_j^+ &= E \psi_j^+ \end{aligned} \quad (\text{B10})$$

By the commensurate approximation, we approximate the irrational number α by the commensurate size, then L becomes the size of the unit cell and the system exhibits the periodic structure. Then to calculate the characteristic polynomial $P(E) = \det |H - EI|$, we can perform the Fourier transformation, i.e. we multiply by $e^{i2\pi\alpha jm}$ and sum over j , then finding characteristic polynomial $P(E) = \det |H - EI|$ becomes finding the determinant $P(E) = \det |A(E)|$, with $A(E)$ being

$$A = \begin{pmatrix} A_{11} & A_{12} & \dots & A_{L1} \\ A_{21} & \ddots & & \vdots \\ \vdots & & \ddots & \vdots \\ A_{L1} & \dots & \dots & A_{LL} \end{pmatrix}_{2L \times 2L},$$

by denoting the hopping coefficients $t_j^\pm = p_j^z \pm i p_j^\perp$, each block being a 2-by-2 matrix as

$$A_{mj} = e^{i2\pi\alpha jm} \begin{pmatrix} t_{j-1}^+ e^{-i(2\pi\alpha m + k_x)} + t_j^{+*} e^{i(2\pi\alpha m + k_x)} + m_j & -E \\ -E & t_{j-1}^- e^{-i(2\pi\alpha m + k_x)} + t_j^{-*} e^{i(2\pi\alpha m + k_x)} + m_j \end{pmatrix} \quad (\text{B11})$$

This form has the advantages that within each element, the energy term E is decoupled from the hopping p_j and on-site term m_j , facilitating the discussion.

To prove that in this case, the system exhibits pure phase with MEs, we are going to prove that the effective coefficients of the dispersion as the we iterating the commensurate approximated system size L will saturate to a energy-independent parameter. First of all, due to the presence of the chiral symmetry, the spectrum of the system is symmetric in energy E with respect to zero energy. Therefore the characteristic polynomial $P(E) = \det |A|$ can only be the polynomial of energy E with even power. In addition, due to the periodic structure of the Hamiltonian, the characteristic polynomial is the function of Lk_x and Lk_y . Now we consider the case of odd L .

We first prove the coefficients that give rise to extended and localized states are energy independent. We first investigate the parameters attached to the leading dispersion $\cos Lk_x$ and $\cos Lk_y$. Since each term within the determinant is obtained by a multiply of $2L$ terms, the terms consisting $\cos Lk_x$ comes from the multiplication of L folds e^{ik_x} and L folds energies E . This indicates that such terms are illegal under the chiral symmetry since such term is of odd power of energy $\sim E^L \cos Lk_x$, which is also the same for $\cos k_y$. So the parameters associated with dispersion $\cos Lk_x$ and $\cos Lk_y$ vanish. Then

the coefficients that give rise to extended and localized states, become the parameters along with the dispersion $\cos 2Lk_x$ and $\cos 2Lk_y$. These two terms can only be obtained by multiply all the diagonal terms in $\det A$, therefore they are energy independent.

Now we prove the parameters associated with the critical states, which are linked to the dispersion $\cos n_x Lk_x \cos n_y Lk_y$ with $n_x, n_y \geq 1 \in \mathbb{Z}$, are also energy independent. Since we are considering the case $p_j^x/p_j^y = \text{Const.} \in \mathbb{R}$ and M_j are purely quasiperiodic, there are basically two choices for the form of the hopping coupling matrix Π_j : One is that the hopping coupling matrix Π_j are uniform while the on-site matrix M_j are purely quasiperiodic. And the other choice is that both Π_j and M_j are purely quasiperiodic.

We first prove that for the case Π_j are uniform, the coefficient associated with $\cos Lk_x \cos Lk_y$ is energy independent. This is because the dispersion $\cos Lk_x \cos Lk_y$ comes from the product of combination of L folds p_j terms and combination of L folds m_j terms, which contribute to L folds e^{ik_x} and e^{ik_y} , respectively. Then the total multiplication of $2L$ elements contribute the $\cos Lk_x \cos Lk_y$, leaving no chance for involving E .

Then we consider the case both Π_j and M_j are purely quasiperiodic, in which case the leading dispersion is $\cos 2Lk_x \cos Lk_y$, $\cos Lk_x \cos 2Lk_y$ or $\cos 2Lk_x \cos 2Lk_y$, whose coefficients are all energy independent. A key

ingredient is that the hopping coupling matrix exhibits the off-diagonal modulation ($V_j^{\text{od}} c_{j+1s}^\dagger c_{js'} + \text{h.c.}$), which makes the p_j contributes the k_x and k_y simultaneously. Therefore, if Π_j are quasiperiodic, $\cos Lk_x \cos Lk_y$ dispersion will disappear. The reason is that $\cos Lk_x \cos Lk_y$ comes from the multiplication of L folds p_j terms and L folds E terms, which is not allowed under the chiral symmetry. So the leading order contributing to the critical orbital in this case is $\cos Lk_x \cos 2Lk_y$ or $\cos 2Lk_x \cos Lk_y$. The first case corresponds multiplication of L folds p_j terms and L folds m_j terms, which are in total $2L$ terms and leaves no chance to involve the extra terms. So the coefficients associated with $\cos Lk_x \cos Lk_y$ are energy independent. Similarly, the $\cos 2Lk_x \cos Lk_y$ originates from the product of $2L$ folds p_j terms. Generically this will lead to $\cos 2Lk_x \cos Lk_y$ and $\cos 2Lk_x \cos 2Lk_y$, and both of them are energy independent. It worthwhile to note that the former one comes from the destruction of relative phases, which gives rise to the $\cos 2Lk_x \cos Lk_y$.

Appendix C: Generalized 2D bilayer mapping

In this section, we provide the detail of the mapping the spinful QP model to a generalized 2D bilayer square lattice system, in the presence of an external magnetic field with an irrational flux threading each unit cell. We provide the detail that the uniform and QP hopping couplings in Π_j are mapped to the hopping couplings along x -direction and diagonal directions, respectively. And the uniform and QP on-site coupling in M_j are mapped to on-site coupling and hopping along y -direction, respectively. This mapping is done by interpreting the phase shift k_y as the quasi-momentum in the y -direction and the spin index s as the layer index. Performing a Fourier transformation, the coefficient V_j^{od} in hopping coupling matrix Π_j and V_j^{d} in the on-site matrix M_j contribute the hopping terms along diagonal and y -directions, respectively. In the following, we analyze this generalized mapping of different processes.

Under the 2D mapping, the uniform hopping coupling $t^{ss'} (c_{j+1s}^\dagger c_{js'} + \text{h.c.})$ in the Hamiltonian characterizes the intra-layer (for $s = s'$) or inter-layer (for $s \neq s'$) hopping coupling in the x -direction

$$t^{ss'} (a_{x+1,y,s}^\dagger a_{x,y,s'} + \text{h.c.}), \quad (\text{C1})$$

with $t^{ss'}$ being the uniform hopping coefficients of different elements in Π_j .

The QP hopping term $\mu^{ss'} V_j^{\text{od}} (c_{j+1s}^\dagger c_{js'} + \text{h.c.})$ in the Hamiltonian characterizes the intra-layer or inter-layer hopping coupling in the diagonal direction in the presence of magnetic flux, which is given by

$$\begin{aligned} & \frac{\mu^{ss'}}{2} (e^{-i2\pi\alpha x} a_{x+1,y+1,s}^\dagger a_{x,y,s'} + \\ & + e^{i2\pi\alpha x} a_{x+1,y-1,s}^\dagger a_{x,y,s'} + \text{h.c.}), \end{aligned} \quad (\text{C2})$$

where $\mu^{ss'}$ are the QP hopping coefficients of different components.

For the uniform on-site coupling $\lambda^{ss'} c_{js}^\dagger c_{js'}$, we obtain the uniform on-site term in the 2D map-ping. When $s = s'$, it characterizes the on-site energy shift, when $s \neq s'$, it denotes the magnitude of on-site inter-layer coupling, which is given by

$$\lambda^{ss'} (a_{x,y,s}^\dagger a_{x,y,s'} + \text{h.c.}). \quad (\text{C3})$$

Finally the QP on-site coupling $V^{ss'} V_j^{\text{d}} c_{js}^\dagger c_{js'}$ characterizes the intra-layer or inter-layer hopping coupling in the y -direction under the magnetic field, with $V^{ss'}$ being the hopping coefficients

$$\frac{V^{ss'}}{2} (e^{-i2\pi\alpha x} a_{x,y+1,s}^\dagger a_{x,y,s'} + \text{h.c.}). \quad (\text{C4})$$

From the analysis above, we can see in the 2D bilayer square lattice, when the hopping along the x - or y -direction dominates, the extended or the localized states emerge. In contrast, the critical states are resulted when the diagonal hopping dominate, with delocalization occurs in both two directions.

Appendix D: Exact solvability of QP systems from local constraint

Now we show the exact solvability for the spinful quasiperiodic system when the hopping coupling matrices satisfy the condition

$$\det |\Pi_j| = 0 \quad \text{or} \quad \det |\Pi_n| = 0, \quad (\text{D1})$$

with off-diagonal terms of M_j being purely constant or purely quasiperiodic.

We first consider the constraint for spin-conserved process, in which case the hopping coupling matrix after the local unitary transformation is given by

$$\tilde{\Pi}_j = \begin{pmatrix} 1 & 0 \\ 0 & 0 \end{pmatrix}. \quad (\text{D2})$$

Without losing generality, we set $t = 1$ here, then the eigenvalue equations $H|\Psi\rangle = E|\Psi\rangle$ with generic on-site coupling matrix M_j become

$$\begin{aligned} u_{j-1\uparrow} + u_{j+1\uparrow} + M_j^{11} u_{j\uparrow} + M_j^{12} u_{j\downarrow} &= E u_{j\uparrow}, \\ M_j^{21} u_{j\uparrow} + M_j^{22} u_{j\downarrow} &= E u_{j\downarrow}. \end{aligned} \quad (\text{D3})$$

Notice that here $u_{j\uparrow}$ and $u_{j\downarrow}$ refer to the coefficients of the wavefunction of the dressed particle after the unitary transformation. We can then obtain the reduced eigenvalue equation

$$u_{j-1\uparrow} + u_{j+1\uparrow} + \left(M_j^{11} + \frac{|M_j^{12}|^2}{E - M_j^{22}} \right) u_{j\uparrow} = E u_{j\uparrow}, \quad (\text{D4})$$

which describe the effective motion with nearest-neighbor hopping and the effective on-site potential is energy dependently dressed by the local modulation from the accompanied internal degree of freedom.

From this expression, we can also see the reason why we require the off-diagonal terms of M_j being purely QP or purely constant. If the off-diagonal terms of M_j contain a constant plus a QP term, then its square will contain both a single QP frequency and double QP frequency, which generically is not analytically solvable.

We then investigate the constraint for spin-conserved process, in which case the hopping coupling matrix after the local unitary transformation is given by

$$\tilde{\Pi}_j = \begin{pmatrix} 0 & 1 \\ 0 & 0 \end{pmatrix}, \quad (\text{D5})$$

$$\frac{M_j^{21}}{E - M_j^{22}} u_{j-1\uparrow} + \frac{M_j^{12}}{E - M_j^{22}} u_{j+1\uparrow} + \left(M_j^{11} + \frac{1}{E - M_j^{22}} + \frac{|M_j^{12}|^2}{E - M_j^{22}} \right) u_{j\uparrow} = E u_{j\uparrow}, \quad (\text{D7})$$

which describes the the effective hopping and on-site potentials are energy dependently dressed by the transfer and local modulation of the accompanied internal degree of freedom.

For the combination of both are similar, where the hopping coupling matrix is given by

$$\tilde{\Pi}_j = \begin{pmatrix} 1 & 1 \\ 0 & 0 \end{pmatrix}, \quad (\text{D8})$$

Similarly we we set both $t = 1$ and $\mu = 1$, then the

$$\left(1 + \frac{M_j^{12}}{E - M_j^{22}} \right) u_{j-1\uparrow} + \left(1 + \frac{M_{j+1}^{21}}{E - M_{j+1}^{22}} \right) u_{j+1\uparrow} + \left(M_j^{11} + \frac{1}{E - M_{j+1}^{22}} + \frac{M_j^{12} M_j^{21}}{E - M_{j+1}^{22}} \right) u_{j\uparrow} = E u_{j\uparrow}. \quad (\text{D10})$$

Appendix E: 1D QP mosaic model

In this section, we introduce the one-dimensional quasiperiodic mosaic model [19, 37] and rewrite it into our 1D spinful QP framework. The generic QP mosaic lattice refers that the modulation of on-site potential and hopping coefficients are in a mosaic manner, namely the the QP modulation or the uniform modulation only appears every κ sites, as we will see in the following.

The original type-I and type-II QP mosaic model is distinguished by the presence of alternating mosaic pattern in hopping coefficients. If the QP modulation only exhibits in the on-site potential, then the mosaic models

Again we we set $\mu = 1$ here for simplicity, then the eigenvalue equations $H|\psi\rangle = E|\psi\rangle$ with generic on-site coupling matrix M_j become

$$\begin{aligned} u_{j-1\downarrow} + M_j^{11} u_{j\uparrow} + M_j^{12} u_{j\downarrow} &= E u_{j\uparrow}, \\ u_{j+1\uparrow} + M_j^{21} u_{j\uparrow} + M_j^{22} u_{j\downarrow} &= E u_{j\downarrow}. \end{aligned} \quad (\text{D6})$$

Then the effective eigen-equation for one for the species is

eigenvalue equations $H|\psi\rangle = E|\psi\rangle$ with generic on-site coupling matrix M_j become

$$\begin{aligned} u_{j+1\uparrow} + u_{j+1\downarrow} + u_{j-1\uparrow} + M_j^{11} u_{j\uparrow} + M_j^{12} u_{j\downarrow} &= E u_{j\uparrow}, \\ u_{j-1\uparrow} + M_j^{21} u_{j\uparrow} + M_j^{22} u_{j\downarrow} &= E u_{j\downarrow}. \end{aligned} \quad (\text{D9})$$

And the effective eigen-equation becomes

belongs to type-I, with Hamiltonian [19]

$$H = \lambda \sum_j (c_j^\dagger c_{j+1} + \text{h.c.}) + 2 \sum_j V_j c_j^\dagger c_j, \quad (\text{E1})$$

where the on-site potential is given by

$$V_j = \begin{cases} V_0 \cos(2\pi\alpha j + \theta), & j = 0 \pmod{\kappa}, \\ 0, & j \neq 0 \pmod{\kappa}. \end{cases} \quad (\text{E2})$$

Here c_j is the annihilation operator at site j , and λ , V , and θ denote the nearest-neighbor hopping coefficient, on-site potential amplitude, and phase offset, respectively. α is an irrational number, and κ is an integer. The QP potential periodically occurs every κ sites.

If the system exhibits QP mosaic modulation in hopping coefficients, then it belongs to type-II QP mosaic

model, with Hamiltonian [37]

$$H = \sum_j (t_j c_j^\dagger c_{j+1} + \text{H.c.}) + \sum_j V_j c_j^\dagger c_j, \quad (\text{E3})$$

here both the quasiperiodic hopping coefficient t_j and on-site potential V_j are in mosaic manners, with the hopping coefficient given by

$$t_j = \begin{cases} 2t \cos(2\pi\alpha j + \theta), & j = 0 \bmod \kappa, \\ \lambda, & j = 1 \bmod \kappa, \\ \lambda, & \text{otherwise,} \end{cases} \quad (\text{E4})$$

and the on-site potential given by

$$V_j = \begin{cases} 2t \cos(2\pi\alpha j + \theta), & j = 0 \bmod \kappa, \\ 2t \cos[2\pi\alpha(j-1) + \theta], & j = 1 \bmod \kappa, \\ 0, & \text{otherwise.} \end{cases} \quad (\text{E5})$$

The conditions for the different states of the two QP mosaic models are summarized in Table V, and the MEs separating different types of states can be obtained accordingly. The critical state is absent in type-I model and the extended state is absent in type-II model. The critical states in the Type II QP mosaic model are generated by the IDZs in the hopping coefficients [37].

	Extended	Critical	Localized
Type I	$E < \lambda^2/V_0 $	none	$E > \lambda^2/V_0 $
Type II	none	$E < \lambda $	$E > \lambda $

Table V. The criteria for different states of type I and type II mosaic models. Here E is the eigenenergies of the system, λ and V_0 are the coefficients defined in the main text. The critical state is absent in type I model and the extended state is absent in type II model.

If we focus on the case $\kappa = 2$, then both two QP mosaic lattice models exhibit a even-odd sublattice structure, which can be rewritten as the spinful QP chain model. We can relabel the even and odd site as spin-up and spin-down degrees of freedom and further relabel the site index, then the Hamiltonian can be rewritten as

$$H_M = \sum_j \lambda (c_{j+1}^\dagger \sigma_- c_j + \text{h.c.}) + \sum_j c_j^\dagger V_j^M c_j, \quad (\text{E6})$$

where $c_j = (c_{j,\uparrow}, c_{j,\downarrow})^\top$ is the spinor for the annihilation operators. The parameter V_j^M controls the type-I and type-II QP mosaic lattice, which respectively given by

$$V_j^{M,I} = 2V_0 V_j^d \Lambda_+ + \lambda \sigma_x, \quad (\text{E7})$$

$$V_j^{M,II} = 2t V_j^d (\sigma_0 + \sigma_x). \quad (\text{E8})$$

Appendix F: Experimental Scheme

In this section, we provide a more detailed description of the experimental scheme for realizing the Hamiltonian

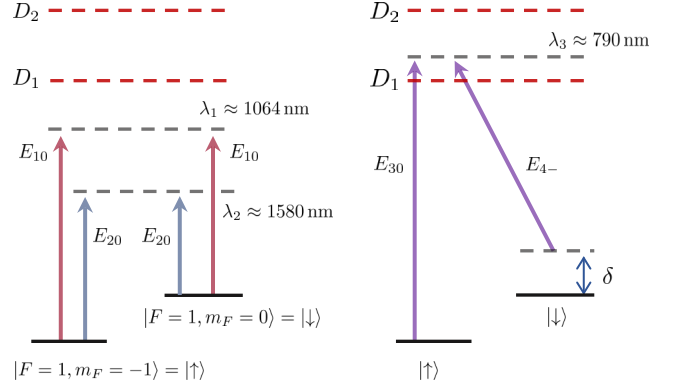


Figure 7. The proposed laser configuration enables the realization of a model featuring all three fundamental types of mobility edges. Laser beams \mathbf{E}_1 and \mathbf{E}_2 with wavelengths λ_1 and λ_2 individually generate spin-independent lattices, while \mathbf{E}_3 and \mathbf{E}_4 operating at ‘tune-out’ wavelength λ_3 form a periodic Raman potential (^{87}Rb atoms).

Eq. (55) in the main text. Without loss of generality, we consider $|\uparrow\rangle \equiv |F=1, m_F=-1\rangle$ and $|\downarrow\rangle \equiv |1, 0\rangle$ of ^{87}Rb atoms as an example, while all results remain applicable to other alkali atoms. After applying the unitary transformation $\sigma_z \rightarrow \sigma_x$ and $\sigma_x \rightarrow -\sigma_z$, the target Hamiltonian can be rewritten as

$$H = \left[\frac{p_z^2}{2m} + \mathcal{V}_s(z) \right] \otimes \sigma_0 + \mathcal{V}_p(z) (\sigma_0 - \sigma_x) / 2 - M_0 \sigma_z, \quad (\text{F1})$$

where $\mathcal{V}_p(z)$ and $\mathcal{V}_s(z)$ represent the primary and secondary optical lattices, respectively. These lattices are generated by two sets of standing waves and a periodic Raman potential. To construct the secondary lattice, we require a standing wave of the form

$$\mathbf{E}_1 = 2E_1 \hat{e}_x e^{i(\phi_1 + \phi'_1/2)} \cos(k_1 z - \phi'_1/2), \quad (\text{F2})$$

where ϕ_1 is the initial phase of the incident beam, and ϕ'_1 is an additional phase acquired by \mathbf{E}_1 before being reflected back to the atoms. Given that the modulus of the wave vector is $k_1 = 2\pi/\lambda_1$, and ignoring the overall constant energy shift, the standing wave field \mathbf{E}_1 induces a spin-independent potential given by

$$\mathcal{V}_1(z) = \frac{V_1}{2} \cos(2k_1 z - \phi'_1), \quad (\text{F3})$$

where

$$V_1 = \sum_{J, F', m'_F} \frac{|\Omega_{F', m'_F; \sigma, 10}^{(J)}|^2}{\Delta_{F', m'_F}^{(J)}}. \quad (\text{F4})$$

In the above, the transition matrix elements are $\Omega_{F', m'_F; \sigma, nq}^{(J)} = -\langle F', m'_F | \mathbf{d} | \sigma \rangle E_n / \hbar$ and $\Delta_{F', m'_F}^{(J)}$ are detunings of laser field from different levels. Here, $J =$

$1/2, 3/2$ correspond to the D_1 and D_2 lines respectively, and $\sigma = \uparrow, \downarrow$ labels the spin states. The index n denotes the laser beam, while $q = 0, \pm$ represents the polarization of laser field. For a laser wavelength of $\lambda_1 \approx 1064$ nm, the overall optical shifts induced by the linearly polarized ($q = 0$) field from \mathbf{E}_1 are nearly identical for the two spin states. Comparing this with Eq. (55), we find

$$k_s = 2k_1, V_s = V_1/2, \phi_s = -\phi'_1. \quad (\text{F5})$$

On the other hand, the primary lattice $\mathcal{V}_p(z)$ is introduced through three laser fields, given by

$$\begin{aligned} \mathbf{E}_2 &= 2E_2 \hat{e}_x e^{i(\phi_2 + \frac{\phi'_2}{2})} \cos\left(k_2 z - \frac{\phi'_2}{2}\right), \\ \mathbf{E}_3 &= 2E_3 \hat{e}_x e^{i(\phi_3 + \frac{\phi'_3}{2})} \cos\left(k_3 z - \frac{\phi'_3}{2}\right), \\ \mathbf{E}_4 &= E_4 \hat{e}_z e^{-ik_3 y + i\phi_4}. \end{aligned} \quad (\text{F6})$$

We first define the spin-independent part of the primary lattice $\mathcal{V}_p(z)$ as a periodic potential generated by the standing wave \mathbf{E}_2 , given by

$$\mathcal{V}_p(z) = \frac{V_2}{2} \cos(2k_2 z - \phi'_2), \quad (\text{F7})$$

where

$$V_2 = \sum_{J, F', m'_F} \frac{\left| \Omega_{F', m'_F; \sigma, 20}^{(J)} \right|^2}{\Delta_{F', m'_F}^{(J)}}. \quad (\text{F8})$$

Then the standing wave \mathbf{E}_3 and the traveling wave \mathbf{E}_4 together generate a periodic Raman potential along the z -direction

$$\mathcal{V}_p(z) = M_{34} e^{i(\phi_4 - \phi_3 - \phi'_3/2)} \cos(k_3 z - \phi'_3/2), \quad (\text{F9})$$

with M_{34} given by

$$M_{34} = \sum_{J, F', m'_F} \frac{\Omega_{F', m'_F; \uparrow, 30}^{(J)*} \Omega_{F', m'_F; \downarrow, 4-}^{(J)}}{\sqrt{2} \Delta_{F', m'_F}^{(J)}}. \quad (\text{F10})$$

Here, we adopt the following gauge convention for the spherical basis: $\hat{e}_z = -1(\hat{e}_+ - \hat{e}_-)/\sqrt{2}$ and $\hat{e}_y = i(\hat{e}_+ + \hat{e}_-)/\sqrt{2}$. For simplicity, we choose ‘tune-out’ wavelength $\lambda_3 \approx 790$ nm [116]. As a result, the lattice depth generated by \mathbf{E}_3 is nearly zero, since the optical shifts from the D_1 and D_2 lines cancel each other out [117]. By comparing this expression with Eq. (F7), the following identities hold:

$$k_3 = 2k_2, M_{34} = V_2/2, \phi'_3/2 = \phi'_2. \quad (\text{F11})$$

The exponential phase factor $\phi_4 - \phi_3 - \phi'_2 = 0$ can be stabilized by locking the relative phase $\phi_4 - \phi_3$ using a phase-locking technique [95, 118, 119]. The two-photon detuning of Raman coupling is defined as $\delta/2 = (\Delta E + \omega_3 - \omega_4)/2 \equiv M_0$, where ΔE is the energy splitting between $|\uparrow\rangle$ and $|\downarrow\rangle$, typically on the order of tens of MHz and $\omega_{3,4}$ denote the corresponding frequencies of $\mathbf{E}_{3,4}$. The sources for \mathbf{E}_2 and $\mathbf{E}_{3,4}$ can be generated using a Raman fiber laser with second-harmonic generation (SHG) cavity, which provides suitable wavelengths of both λ_2 and $\lambda_{3,4}$ at the same time. The additional phase ϕ'_3 and ϕ'_2 acquired along the reflective path can be finely tuned by varying the optical path length of the reflected beam.

Finally, we see that the QD lattice in Eq. (55) can be realized using the proposed scheme when the following conditions are satisfied:

$$k_p = 2k_2, V_p = V_2/2, \phi_p = -\phi'_2. \quad (\text{F12})$$

This experimental scheme leads to a ratio of $\alpha = k_p/k_s \approx 0.67$. The nearest-neighbor hopping amplitude t , determined by the lattice potential V_0 , approximately follows the relation $t \approx 4V_0^{3/4} e^{-2\sqrt{V_0}}/\sqrt{\pi}$ [13]. To suppress the nearest-neighbor hopping for spin-down atoms, the parameters $V_s = 2.5, V_p = 10, M_0 = 1.5$ are chosen such that the hopping amplitude t for spin-up atoms is about one order of magnitude larger than that for spin-down atoms.

-
- [1] P. W. Anderson, “Absence of Diffusion in Certain Random Lattices,” *Phys. Rev.* **109**, 1492–1505 (1958).
 - [2] Patrick A. Lee and T. V. Ramakrishnan, “Disordered electronic systems,” *Rev. Mod. Phys.* **57**, 287–337 (1985).
 - [3] B. Kramer and A. MacKinnon, “Localization: Theory and experiment,” *Rep. Prog. Phys.* **56**, 1469 (1993).
 - [4] Ferdinand Evers and Alexander D. Mirlin, “Anderson transitions,” *Rev. Mod. Phys.* **80**, 1355–1417 (2008).
 - [5] E. Abrahams, P. W. Anderson, D. C. Licciardello, and T. V. Ramakrishnan, “Scaling Theory of Localization: Absence of Quantum Diffusion in Two Dimensions,” *Phys. Rev. Lett.* **42**, 673–676 (1979).
 - [6] S. Aubry and G. André, “Analyticity breaking and Anderson localization in incommensurate lattices,” *Ann. Israel Phys. Soc.* **3**, 133 (1980).
 - [7] Giacomo Roati, Chiara D’Errico, Leonardo Fallani, Marco Fattori, Chiara Fort, Matteo Zaccanti, Giovanni

- Modugno, Michele Modugno, and Massimo Inguscio, “Anderson localization of a non-interacting Bose–Einstein condensate,” *Nature* **453**, 895–898 (2008).
- [8] C. M. Soukoulis and E. N. Economou, “Localization in One-Dimensional Lattices in the Presence of Incommensurate Potentials,” *Phys. Rev. Lett.* **48**, 1043–1046 (1982).
- [9] S. Das Sarma, Song He, and X. C. Xie, “Mobility Edge in a Model One-Dimensional Potential,” *Phys. Rev. Lett.* **61**, 2144–2147 (1988).
- [10] Dave J. Boers, Benjamin Goedeke, Dennis Hinrichs, and Martin Holthaus, “Mobility edges in bichromatic optical lattices,” *Phys. Rev. A* **75**, 063404 (2007).
- [11] J. Biddle and S. Das Sarma, “Predicted Mobility Edges in One-Dimensional Incommensurate Optical Lattices: An Exactly Solvable Model of Anderson Localization,” *Phys. Rev. Lett.* **104**, 070601 (2010).
- [12] Sriram Ganeshan, J. H. Pixley, and S. Das Sarma, “Nearest Neighbor Tight Binding Models with an Exact Mobility Edge in One Dimension,” *Phys. Rev. Lett.* **114**, 146601 (2015).
- [13] Xiao Li, Xiaopeng Li, and S. Das Sarma, “Mobility edges in one-dimensional bichromatic incommensurate potentials,” *Phys. Rev. B* **96**, 085119 (2017).
- [14] Sarang Gopalakrishnan, “Self-dual quasiperiodic systems with power-law hopping,” *Phys. Rev. B* **96**, 054202 (2017).
- [15] Fangzhao Alex An, Eric J. Meier, and Bryce Gadway, “Engineering a Flux-Dependent Mobility Edge in Disordered Zigzag Chains,” *Phys. Rev. X* **8**, 031045 (2018).
- [16] Henrik P. Lüschen, Sebastian Scherg, Thomas Kohlert, Michael Schreiber, Pranjal Bordia, Xiao Li, S. Das Sarma, and Immanuel Bloch, “Single-Particle Mobility Edge in a One-Dimensional Quasiperiodic Optical Lattice,” *Phys. Rev. Lett.* **120**, 160404 (2018).
- [17] Thomas Kohlert, Sebastian Scherg, Xiao Li, Henrik P. Lüschen, Sankar Das Sarma, Immanuel Bloch, and Monika Aidelsburger, “Observation of Many-Body Localization in a One-Dimensional System with a Single-Particle Mobility Edge,” *Phys. Rev. Lett.* **122**, 170403 (2019).
- [18] X. Deng, S. Ray, S. Sinha, G. V. Shlyapnikov, and L. Santos, “One-Dimensional Quasicrystals with Power-Law Hopping,” *Phys. Rev. Lett.* **123**, 025301 (2019).
- [19] Yucheng Wang, Xu Xia, Long Zhang, Hepeng Yao, Shu Chen, Jiangong You, Qi Zhou, and Xiong-Jun Liu, “One-Dimensional Quasiperiodic Mosaic Lattice with Exact Mobility Edges,” *Phys. Rev. Lett.* **125**, 196604 (2020).
- [20] Xiao Li and S. Das Sarma, “Mobility edge and intermediate phase in one-dimensional incommensurate lattice potentials,” *Phys. Rev. B* **101**, 064203 (2020).
- [21] Alexander Duthie, Sthitadhi Roy, and David E. Logan, “Self-consistent theory of mobility edges in quasiperiodic chains,” *Phys. Rev. B* **103**, L060201 (2021).
- [22] Fangzhao Alex An, Karmela Padavić, Eric J. Meier, Suraj Hegde, Sriram Ganeshan, J. H. Pixley, Smitha Vishveshwara, and Bryce Gadway, “Interactions and Mobility Edges: Observing the Generalized Aubry-André Model,” *Phys. Rev. Lett.* **126**, 040603 (2021).
- [23] Shilpi Roy, Tapan Mishra, B. Tanatar, and Saurabh Basu, “Reentrant Localization Transition in a Quasiperiodic Chain,” *Phys. Rev. Lett.* **126**, 106803 (2021).
- [24] Nilanjan Roy and Auditya Sharma, “Fraction of delocalized eigenstates in the long-range Aubry-André-Harper model,” *Phys. Rev. B* **103**, 075124 (2021).
- [25] Yucheng Wang, Xu Xia, Yongjian Wang, Zuohuan Zheng, and Xiong-Jun Liu, “Duality between two generalized Aubry-André models with exact mobility edges,” *Phys. Rev. B* **103**, 174205 (2021).
- [26] Yunfei Wang, Jia-Hui Zhang, Yuqing Li, Jizhou Wu, Wenliang Liu, Feng Mei, Ying Hu, Liantuan Xiao, Jie Ma, Cheng Chin, and Suotang Jia, “Observation of Interaction-Induced Mobility Edge in an Atomic Aubry-André Wire,” *Phys. Rev. Lett.* **129**, 103401 (2022).
- [27] Stefano Longhi, “Absence of mobility edges in mosaic Wannier-Stark lattices,” *Phys. Rev. B* **108**, 064206 (2023).
- [28] Yongjian Wang, Xu Xia, Jiangong You, Zuohuan Zheng, and Qi Zhou, “Exact Mobility Edges for 1D Quasiperiodic Models,” *Commun. Math. Phys.* **401**, 2521–2567 (2023).
- [29] Jun Gao, Ivan M. Khaymovich, Adrian Iovan, Xiao-Wei Wang, Govind Krishna, Ze-Sheng Xu, Emrah Tortumlu, Alexander V. Balatsky, Val Zwiller, and Ali W. Elshaari, “Coexistence of extended and localized states in finite-sized mosaic Wannier-Stark lattices,” *Phys. Rev. B* **108**, L140202 (2023).
- [30] Stefano Longhi, “Resonances, mobility edges, and gap-protected Anderson localization in generalized disordered mosaic lattices,” *Phys. Rev. B* **110**, 184201 (2024).
- [31] Stefano Longhi, “Dephasing-Induced Mobility Edges in Quasicrystals,” *Phys. Rev. Lett.* **132**, 236301 (2024).
- [32] Xingbo Wei, Liangqing Wu, Kewei Feng, Tong Liu, and Yunbo Zhang, “Coexistence of ergodic and weakly ergodic states in finite-height Wannier-Stark ladders,” *Phys. Rev. A* **109**, 023314 (2024).
- [33] Jun Gao, Ivan M. Khaymovich, Xiao-Wei Wang, Ze-Sheng Xu, Adrian Iovan, Govind Krishna, Jiayidaer Jieensi, Andrea Cataldo, Alexander V. Balatsky, Val Zwiller, and Ali W. Elshaari, “Probing multi-mobility edges in quasiperiodic mosaic lattices,” *Science Bulletin* (2024), 10.1016/j.scib.2024.09.030.
- [34] Yaru Liu, Zeqing Wang, Chao Yang, Jianwen Jie, and Yucheng Wang, “Dissipation-Induced Extended-Localized Transition,” *Phys. Rev. Lett.* **132**, 216301 (2024).
- [35] Hugo Tabanelli, Claudio Castelnovo, and Antonio Štrkalj, “Reentrant localization transitions and anomalous spectral properties in off-diagonal quasiperiodic systems,” *Phys. Rev. B* **110**, 184208 (2024).
- [36] Toshihiko Shimasaki, Yifei Bai, H. Esat Kondakci, Peter Dotti, Jared E. Pagett, Anna R. Dardia, Max Prichard, André Eckardt, and David M. Weld, “Reversible Phasonic Control of a Quantum Phase Transition in a Quasicrystal,” *Phys. Rev. Lett.* **133**, 083405 (2024).
- [37] Xin-Chi Zhou, Yongjian Wang, Ting-Fung Jeffrey Poon, Qi Zhou, and Xiong-Jun Liu, “Exact New Mobility Edges between Critical and Localized States,” *Phys. Rev. Lett.* **131**, 176401 (2023).
- [38] Miguel Gonçalves, Bruno Amorim, Eduardo V. Castro, and Pedro Ribeiro, “Critical Phase Dualities in 1D Exactly Solvable Quasiperiodic Models,” *Phys. Rev. Lett.* **131**, 186303 (2023).
- [39] Tong Liu, Xu Xia, Stefano Longhi, and Laurent Sanchez-Palencia, “Anomalous mobility edges in one-dimensional quasiperiodic models,” *SciPost Physics* **12**,

- 027 (2022).
- [40] Y. Hatsugai and M. Kohmoto, “Energy spectrum and the quantum Hall effect on the square lattice with next-nearest-neighbor hopping,” *Phys. Rev. B* **42**, 8282–8294 (1990).
- [41] J. H. Han, D. J. Thouless, H. Hiramoto, and M. Kohmoto, “Critical and bicritical properties of Harper’s equation with next-nearest-neighbor coupling,” *Phys. Rev. B* **50**, 11365–11380 (1994).
- [42] D. Tanese, E. Gurevich, F. Baboux, T. Jacqmin, A. Lemaître, E. Galopin, I. Sagnes, A. Amo, J. Bloch, and E. Akkermans, “Fractal Energy Spectrum of a Polariton Gas in a Fibonacci Quasiperiodic Potential,” *Phys. Rev. Lett.* **112**, 146404 (2014).
- [43] Jun Wang, Xia-Ji Liu, Gao Xianlong, and Hui Hu, “Phase diagram of a non-Abelian Aubry-André-Harper model with p -wave superfluidity,” *Phys. Rev. B* **93**, 104504 (2016).
- [44] Fangli Liu, Somnath Ghosh, and Y. D. Chong, “Localization and adiabatic pumping in a generalized Aubry-André-Harper model,” *Phys. Rev. B* **91**, 014108 (2015).
- [45] Qi-Bo Zeng, Shu Chen, and Rong Lü, “Generalized Aubry-André-Harper model with p -wave superconducting pairing,” *Phys. Rev. B* **94**, 125408 (2016).
- [46] Hepeng Yao, Alice Khoudli, Léa Bresque, and Laurent Sanchez-Palencia, “Critical Behavior and Fractality in Shallow One-Dimensional Quasiperiodic Potentials,” *Phys. Rev. Lett.* **123**, 070405 (2019).
- [47] Yucheng Wang, Long Zhang, Sen Niu, Dapeng Yu, and Xiong-Jun Liu, “Realization and Detection of Nonergodic Critical Phases in an Optical Raman Lattice,” *Phys. Rev. Lett.* **125**, 073204 (2020).
- [48] V. Goblot, A. Štrkalj, N. Pernet, J. L. Lado, C. Dorow, A. Lemaître, L. Le Gratiet, A. Harouri, I. Sagnes, S. Ravets, A. Amo, J. Bloch, and O. Zilberberg, “Emergence of criticality through a cascade of delocalization transitions in quasiperiodic chains,” *Nat. Phys.* **16**, 832–836 (2020).
- [49] Teng Xiao, Dizhou Xie, Zhaoli Dong, Tao Chen, Wei Yi, and Bo Yan, “Observation of topological phase with critical localization in a quasi-periodic lattice,” *Science Bulletin* **66**, 2175–2180 (2021).
- [50] Hao Li, Yong-Yi Wang, Yun-Hao Shi, Kaixuan Huang, Xiaohui Song, Gui-Han Liang, Zheng-Yang Mei, Bozhen Zhou, He Zhang, Jia-Chi Zhang, Shu Chen, S. P. Zhao, Ye Tian, Zhan-Ying Yang, Zhongcheng Xiang, Kai Xu, Dongning Zheng, and Heng Fan, “Observation of critical phase transition in a generalized Aubry-André-Harper model with superconducting circuits,” *npj Quantum Inf* **9**, 1–6 (2023).
- [51] Yucheng Wang, Long Zhang, Wei Sun, Ting-Fung Jeffrey Poon, and Xiong-Jun Liu, “Quantum phase with coexisting localized, extended, and critical zones,” *Phys. Rev. B* **106**, L140203 (2022).
- [52] Xiaoshui Lin, Xiaoman Chen, Guang-Can Guo, and Ming Gong, “General approach to the critical phase with coupled quasiperiodic chains,” *Phys. Rev. B* **108**, 174206 (2023).
- [53] Sanghoon Lee, Alexei Andreanov, and Sergej Flach, “Critical-to-insulator transitions and fractality edges in perturbed flat bands,” *Phys. Rev. B* **107**, 014204 (2023).
- [54] Qi Dai, Zhanpeng Lu, and Zhihao Xu, “Emergence of multifractality through cascadelike transitions in a mosaic interpolating Aubry-André-Fibonacci chain,” *Phys. Rev. B* **108**, 144207 (2023).
- [55] Toshihiko Shimasaki, Max Prichard, H. Esat Kondakci, Jared E. Pagett, Yifei Bai, Peter Dotti, Alec Cao, Anna R. Dardia, Tsung-Cheng Lu, Tarun Grover, and David M. Weld, “Anomalous localization in a kicked quasicrystal,” *Nat. Phys.* **20**, 409–414 (2024).
- [56] Xuegang Li, Huikai Xu, Junhua Wang, Ling-Zhi Tang, Dan-Wei Zhang, Chuhong Yang, Tang Su, Chenlu Wang, Zhenyu Mi, Weijie Sun, Xuehui Liang, Mo Chen, Chengyao Li, Yingshan Zhang, Kehuan Linghu, Jiaxiu Han, Weiyang Liu, Yulong Feng, Pei Liu, Guangming Xue, Jingning Zhang, Yirong Jin, Shi-Liang Zhu, Haifeng Yu, S. P. Zhao, and Qi-Kun Xue, “Mapping the topology-localization phase diagram with quasiperiodic disorder using a programmable superconducting simulator,” *Phys. Rev. Res.* **6**, L042038 (2024).
- [57] Yongjian Wang and Qi Zhou, “Exact new mobility edges,” (2025), [arXiv:2501.17523](https://arxiv.org/abs/2501.17523).
- [58] Wenhui Huang, Xin-Chi Zhou, Libo Zhang, Jiawei Zhang, Yuxuan Zhou, Zechen Guo, Bing-Chen Yao, Peisheng Huang, Qixian Li, Yongqi Liang, Yiting Liu, Jiawei Qiu, Daxiong Sun, Xuandong Sun, Zilin Wang, Changrong Xie, Yuzhe Xiong, Xiaohan Yang, Jiajian Zhang, Zihao Zhang, Ji Chu, Weijie Guo, Ji Jiang, Xiayu Linpeng, Wenhui Ren, Yuefeng Yuan, Jingjing Niu, Ziyu Tao, Song Liu, Youpeng Zhong, Xiong-Jun Liu, and Dapeng Yu, “Exact quantum critical states with a superconducting quantum processor,” (2025), [arXiv:2502.19185](https://arxiv.org/abs/2502.19185).
- [59] Wen Chen, Pedro D. Sacramento, and Rubem Mondaini, “Multifractality and prethermalization in the quasiperiodically kicked Aubry-André-Harper model,” *Phys. Rev. B* **109**, 054202 (2024).
- [60] Chenyue Guo, “Multiple intermediate phases in the interpolating Aubry-André-Fibonacci model,” *Phys. Rev. B* **109**, 174203 (2024).
- [61] Peter Dotti, Yifei Bai, Toshihiko Shimasaki, Anna R. Dardia, and David M. Weld, “Measuring a localization phase diagram controlled by the interplay of disorder and driving,” (2024), [arXiv:2406.00214](https://arxiv.org/abs/2406.00214).
- [62] Chao Yang, Weizhe Yang, Yongjian Wang, and Yucheng Wang, “Exploring multifractal critical phases in two-dimensional quasiperiodic systems,” *Phys. Rev. A* **110**, 042205 (2024).
- [63] Callum W. Duncan, “Critical states and anomalous mobility edges in two-dimensional diagonal quasicrystals,” *Phys. Rev. B* **109**, 014210 (2024).
- [64] Qi Yao, Xiaotian Yang, Askar A. Iliasov, Mikhail I. Katsnelson, and Shengjun Yuan, “Wave functions in the critical phase: A planar Sierpinski fractal lattice,” *Phys. Rev. B* **110**, 035403 (2024).
- [65] Yifei Bai and David M. Weld, “Tunably polarized driving light controls the phase diagram of one-dimensional quasicrystals and two-dimensional quantum Hall matter,” *Phys. Rev. B* **111**, 115163 (2025).
- [66] Artur Avila, “Global theory of one-frequency Schrödinger operators,” *Acta Mathematica* **215**, 1–54 (2015).
- [67] Barry Simon and Thomas Spencer, “Trace class perturbations and the absence of absolutely continuous spectra,” *Commun. Math. Phys.* **125**, 113–125 (1989).
- [68] S. Jitomirskaya and C. A. Marx, “Analytic Quasi-

- Periodic Cocycles with Singularities and the Lyapunov Exponent of Extended Harper's Model," *Commun. Math. Phys.* **316**, 237–267 (2012).
- [69] Xiong-Jun Liu, "Quantum matter in multifractal patterns," *Nat. Phys.* , 1–2 (2024).
- [70] M. V. Feigel'man, L. B. Ioffe, V. E. Kravtsov, and E. A. Yuzbashyan, "Eigenfunction Fractality and Pseudogap State near the Superconductor-Insulator Transition," *Phys. Rev. Lett.* **98**, 027001 (2007).
- [71] I. S. Burmistrov, I. V. Gornyi, and A. D. Mirlin, "Enhancement of the Critical Temperature of Superconductors by Anderson Localization," *Phys. Rev. Lett.* **108**, 017002 (2012).
- [72] Kun Zhao, Haicheng Lin, Xiao Xiao, Wantong Huang, Wei Yao, Mingzhe Yan, Ying Xing, Qinghua Zhang, Zi-Xiang Li, Shintaro Hoshino, Jian Wang, Shuyun Zhou, Lin Gu, Mohammad Saeed Bahrany, Hong Yao, Naoto Nagaosa, Qi-Kun Xue, Kam Tuen Law, Xi Chen, and Shuai-Hua Ji, "Disorder-induced multifractal superconductivity in monolayer niobium dichalcogenides," *Nat. Phys.* **15**, 904–910 (2019).
- [73] Benjamin Sacépé, Mikhail Feigel'man, and Teunis M. Klapwijk, "Quantum breakdown of superconductivity in low-dimensional materials," *Nat. Phys.* **16**, 734–746 (2020).
- [74] Miguel Gonçalves, Bruno Amorim, Flavio Riche, Eduardo V. Castro, and Pedro Ribeiro, "Incommensurability enabled quasi-fractal order in 1D narrow-band moiré systems," *Nat. Phys.* , 1–8 (2024).
- [75] Yucheng Wang, Chen Cheng, Xiong-Jun Liu, and Dapeng Yu, "Many-Body Critical Phase: Extended and Nonthermal," *Phys. Rev. Lett.* **126**, 080602 (2021).
- [76] Arijee Pal and David A. Huse, "Many-body localization phase transition," *Phys. Rev. B* **82**, 174411 (2010).
- [77] Rahul Nandkishore and David A. Huse, "Many-Body Localization and Thermalization in Quantum Statistical Mechanics," *Annual Review of Condensed Matter Physics* **6**, 15–38 (2015).
- [78] Michael Schreiber, Sean S. Hodgman, Pranjal Bordia, Henrik P. Lüschen, Mark H. Fischer, Ronen Vosk, Ehud Altman, Ulrich Schneider, and Immanuel Bloch, "Observation of many-body localization of interacting fermions in a quasirandom optical lattice," *Science* **349**, 842–845 (2015).
- [79] Pranjal Bordia, Henrik P. Lüschen, Sean S. Hodgman, Michael Schreiber, Immanuel Bloch, and Ulrich Schneider, "Coupling Identical one-dimensional Many-Body Localized Systems," *Phys. Rev. Lett.* **116**, 140401 (2016).
- [80] Pranjal Bordia, Henrik Lüschen, Sebastian Scherg, Sarang Gopalakrishnan, Michael Knap, Ulrich Schneider, and Immanuel Bloch, "Probing Slow Relaxation and Many-Body Localization in Two-Dimensional Quasiperiodic Systems," *Phys. Rev. X* **7**, 041047 (2017).
- [81] Henrik P. Lüschen, Pranjal Bordia, Sebastian Scherg, Fabien Alet, Ehud Altman, Ulrich Schneider, and Immanuel Bloch, "Observation of Slow Dynamics near the Many-Body Localization Transition in One-Dimensional Quasiperiodic Systems," *Phys. Rev. Lett.* **119**, 260401 (2017).
- [82] Pranjal Bordia, Henrik Lüschen, Ulrich Schneider, Michael Knap, and Immanuel Bloch, "Periodically driving a many-body localized quantum system," *Nature Phys* **13**, 460–464 (2017).
- [83] Luca D'Alessio, Yariv Kafri, Anatoli Polkovnikov, and Marcos Rigol, "From quantum chaos and eigenstate thermalization to statistical mechanics and thermodynamics," *Advances in Physics* (2016).
- [84] J. M. Deutsch, "Quantum statistical mechanics in a closed system," *Phys. Rev. A* **43**, 2046–2049 (1991).
- [85] Marcos Rigol, Vanja Dunjko, and Maxim Olshanii, "Thermalization and its mechanism for generic isolated quantum systems," *Nature* **452**, 854–858 (2008).
- [86] Mark Srednicki, "Chaos and quantum thermalization," *Phys. Rev. E* **50**, 888–901 (1994).
- [87] Xiaoshui Lin and Ming Gong, "Fate of localization in a coupled free chain and a disordered chain," *Phys. Rev. A* **109**, 033310 (2024).
- [88] Long Zhang and Xiong-Jun Liu, "Spin-orbit Coupling and Topological Phases for Ultracold Atoms," in *Synthetic Spin-Orbit Coupling in Cold Atoms* (WORLD SCIENTIFIC, 2018) pp. 1–87.
- [89] Xiong-Jun Liu, K. T. Law, and T. K. Ng, "Realization of 2D Spin-Orbit Interaction and Exotic Topological Orders in Cold Atoms," *Phys. Rev. Lett.* **112**, 086401 (2014).
- [90] Zhan Wu, Long Zhang, Wei Sun, Xiao-Tian Xu, Bao-Zong Wang, Si-Cong Ji, Youjin Deng, Shuai Chen, Xiong-Jun Liu, and Jian-Wei Pan, "Realization of two-dimensional spin-orbit coupling for Bose-Einstein condensates," *Science* **354**, 83–88 (2016).
- [91] Bao-Zong Wang, Yue-Hui Lu, Wei Sun, Shuai Chen, Youjin Deng, and Xiong-Jun Liu, "Dirac-, Rashba-, and Weyl-type spin-orbit couplings: Toward experimental realization in ultracold atoms," *Phys. Rev. A* **97**, 011605 (2018).
- [92] Wei Sun, Bao-Zong Wang, Xiao-Tian Xu, Chang-Rui Yi, Long Zhang, Zhan Wu, Youjin Deng, Xiong-Jun Liu, Shuai Chen, and Jian-Wei Pan, "Highly Controllable and Robust 2D Spin-Orbit Coupling for Quantum Gases," *Phys. Rev. Lett.* **121**, 150401 (2018).
- [93] Bo Song, Chengdong He, Sen Niu, Long Zhang, Zejian Ren, Xiong-Jun Liu, and Gyu-Boong Jo, "Observation of nodal-line semimetal with ultracold fermions in an optical lattice," *Nat. Phys.* **15**, 911–916 (2019).
- [94] Yue-Hui Lu, Bao-Zong Wang, and Xiong-Jun Liu, "Ideal Weyl semimetal with 3D spin-orbit coupled ultracold quantum gas," *Science Bulletin* **65**, 2080–2085 (2020).
- [95] Zong-Yao Wang, Xiang-Can Cheng, Bao-Zong Wang, Jin-Yi Zhang, Yue-Hui Lu, Chang-Rui Yi, Sen Niu, Youjin Deng, Xiong-Jun Liu, Shuai Chen, and Jian-Wei Pan, "Realization of an ideal Weyl semimetal band in a quantum gas with 3D spin-orbit coupling," *Science* **372**, 271–276 (2021).
- [96] Han Zhang, Wen-Wei Wang, Chang Qiao, Long Zhang, Ming-Cheng Liang, Rui Wu, Xu-Jie Wang, Xiong-Jun Liu, and Xibo Zhang, "Topological spin-orbit-coupled fermions beyond rotating wave approximation," *Science Bulletin* **69**, 747–755 (2024).
- [97] Yaacov E. Kraus and Oded Zeitlinger, "Topological Equivalence between the Fibonacci Quasicrystal and the Harper Model," *Phys. Rev. Lett.* **109**, 116404 (2012).
- [98] Dan S. Borgnia and Robert-Jan Slager, "Localization as a consequence of quasiperiodic bulk-bulk correspondence," *Phys. Rev. B* **107**, 085111 (2023).
- [99] M Suslov, "Localization in one-dimensional incommensurate systems," *Sov. Phys. JETP* **56**, 612 (1982).

- [100] D. J. Thouless and Q. Niu, “Wavefunction scaling in a quasi-periodic potential,” *J. Phys. A: Math. Gen.* **16**, 1911 (1983).
- [101] Stellan Ostlund and Rahul Pandit, “Renormalization-group analysis of the discrete quasiperiodic Schrödinger equation,” *Phys. Rev. B* **29**, 1394–1414 (1984).
- [102] Qian Niu and Franco Nori, “Renormalization-Group Study of One-Dimensional Quasiperiodic Systems,” *Phys. Rev. Lett.* **57**, 2057–2060 (1986).
- [103] Qian Niu and Franco Nori, “Spectral splitting and wave-function scaling in quasicrystalline and hierarchical structures,” *Phys. Rev. B* **42**, 10329–10341 (1990).
- [104] Attila Szabó and Ulrich Schneider, “Non-power-law universality in one-dimensional quasicrystals,” *Phys. Rev. B* **98**, 134201 (2018).
- [105] Anuradha Jagannathan, “The Fibonacci quasicrystal: Case study of hidden dimensions and multifractality,” *Rev. Mod. Phys.* **93**, 045001 (2021).
- [106] Miguel Gonçalves, Bruno Amorim, Eduardo Castro, and Pedro Ribeiro, “Hidden dualities in 1D quasiperiodic lattice models,” *SciPost Physics* **13**, 046 (2022).
- [107] Miguel Gonçalves, B. Amorim, Eduardo V. Castro, and Pedro Ribeiro, “Renormalization group theory of one-dimensional quasiperiodic lattice models with commensurate approximants,” *Phys. Rev. B* **108**, L100201 (2023).
- [108] The dispersion $\cos Lk_x \cos Lk_y$ vanishes due to QP hopping in the hopping coupling matrix, which ensures that p_j contributes $e^{ik_x} e^{ik_y}$. This dispersion arises from the product of L factors of p_j and E , which gives $E^L \cos Lk_x \cos Lk_y$, prohibited by chiral symmetry.
- [109] The $\cos 2Lk_x \cos Lk_y$ term results from the destruction of relative phases in m_j , which gives rise to this dispersion.
- [110] Breaking the chiral symmetry does not necessarily result in mobility edges (MEs). While it enables the possibility of MEs, their existence depends on whether MEs fall within the eigenstates, which is determined by the microscopic details. In other words, even if chiral symmetry is broken, the system remains in a pure phase as long as the MEs do not intersect the spectrum.
- [111] Wade DeGottardi, Diptiman Sen, and Smitha Vishveshwara, “Topological phases, Majorana modes and quench dynamics in a spin ladder system,” *New J. Phys.* **13**, 065028 (2011).
- [112] Wade DeGottardi, Diptiman Sen, and Smitha Vishveshwara, “Majorana Fermions in Superconducting 1D Systems Having Periodic, Quasiperiodic, and Disordered Potentials,” *Phys. Rev. Lett.* **110**, 146404 (2013).
- [113] P. Soltan-Panahi, J. Struck, P. Hauke, A. Bick, W. Plenkers, G. Meineke, C. Becker, P. Windpassinger, M. Lewenstein, and K. Sengstock, “Multi-component quantum gases in spin-dependent hexagonal lattices,” *Nature Physics* **7**, 434–440 (2011).
- [114] Igor Kuzmenko, Tetyana Kuzmenko, Y. Avishai, and Y. B. Band, “Atoms trapped by a spin-dependent optical lattice potential: Realization of a ground-state quantum rotor,” *Phys. Rev. A* **100**, 033415 (2019).
- [115] Piotr Szulim, Marek Trippenbach, Y B Band, Mariusz Gajda, and Mirosław Brewczyk, “Atoms in a spin dependent optical potential: ground state topology and magnetization,” *New Journal of Physics* **24**, 033041 (2022).
- [116] Kai Wen, Zengming Meng, Liangwei Wang, Liangchao Chen, Lianghai Huang, Pengjun Wang, and Jing Zhang, “Experimental study of tune-out wavelengths for spin-dependent optical lattice in ^{87}Rb bose-einstein condensation,” *Journal of the Optical Society of America B* **38**, 3269 (2021).
- [117] The tune-out wavelengths for spin-up and spin-down atoms are slightly different. However, one can always reduce the intensity of the \mathbf{E}_3 field while increasing that of the \mathbf{E}_4 field to further suppress the periodic potential generated by \mathbf{E}_3 , while still ensuring that the condition is satisfied.
- [118] Gregor Jotzu, Michael Messer, Rémi Desbuquois, Martin Lebrat, Thomas Uehlinger, Daniel Greif, and Tilman Esslinger, “Experimental realization of the topological haldane model with ultracold fermions,” *Nature* **515**, 237–240 (2014).
- [119] Frederik Görg, Kilian Sandholzer, Joaquín Minguzzi, Rémi Desbuquois, Michael Messer, and Tilman Esslinger, “Realization of density-dependent peierls phases to engineer quantized gauge fields coupled to ultracold matter,” *Nature Physics* **15**, 1161–1167 (2019).